Evaluation of the Factors Influencing Reactivity and Stereospecificity in NAD(P)H Dependent Dehydrogenase Enzymes

Örn Almarsson[1] and Thomas C. Bruice*

Contribution from the Department of Chemistry, University of California at Santa Barbara, Santa Barbara, California 93106. *Received September 10, 1992*

Abstract: Calculations of AM1 potential energies for conformations of *N*-(1,β-ribosyl)-1,4-dihydronicotinamide (**3H**) and *N*-(1,β-ribosyl)nicotinamide (**3**), as defined by the nicotinamide ring deformation angles α_C and α_N and the torsion angles X_n and X_{am}, have been carried out. X_n is the angle of rotation of the nicotinamide ring relative to the ribose ring and the conformers are designated as *syn* (nicotinamide $-CONH_2$ and ribose ring O are close) and *anti* (nicotinamide $-CONH_2$ and ribose ring O are distant). The angles α_C and α_N reflect the degree of bending of nicotinamide N and C4 out of the plane with C2, C3, C5, and C6 to provide *quasi*-boat and *quasi*-half-chair conformations. With the 1,4-dihydronicotinamide ring in a *quasi*-boat geometry, the relationship of the anti-bonding orbital on the ribose ether O and the unshared electron pair on the nicotinamide ring N is described as periplanar or antiperiplanar. The *quasi*-boat conformations may then be described as *anti* antiperiplanar (**1a**), *syn* antiperiplanar (**1b**), *anti* periplanar (**1c**), and *syn* periplanar (**1d**). The AM1 potential energies expended in the deformation of the 1,4-dihydropyridine ring to *quasi*-boat or *quasi*-half-chair conformations (with $\alpha_C + \alpha_N \leq 20°$ and $\alpha_C \geq \alpha_N$) are less than the gain in the accompanying stabilization of the transition state in the reduction of a carbonyl function by transfer of the pseudoaxial hydrogen at C4. With $\alpha_C = 15°$ and $\alpha_N = 5°$, the potential energies of **3** as a function of X_n is raised relative to its global minimum by an average value of 16 kcal/mol. To bend the flat 1,4-dihydronicotinamide of **3H** such that $\alpha_C = 15°$ and $\alpha_N = 5°$ costs 1.8 kcal/mol, while the activation enthalpy is decreased by 6 kcal/mol compared with the flat nicotinamide. In the bent conformation, the initial state {**3H** + $H_2C{=}O{\cdots}HImH^+$} and immediate product state {**3** + $H_3COH{\cdots}ImH$} potential energies are not greatly different. Energetically, there is little difference as to whether H_R or H_S are the transferred entities at the pseudoaxial positions. From structures deposited in the Brookhaven database, $X_n = -87°$ to $-140°$ (conformation **1a**) for A-specific and $X_n = 45°$ to 66° (conformation **1b**) for B-specific dehydrogenases. The mismatch in the preferred values of X_n for unbound (AM1) and enzyme bound (Brookhaven database) reduced and oxidized cofactors has little influence on the equilibrium constants for cofactor binding which favors the reduced form. $CHARM_m$ molecular dynamics simulations show the deformation of the $\alpha_C + \alpha_N$ of **3H** to A- and B-sides is isoenergetic when **3H** is not enzyme bound. The same experiments with dogfish muscle lactate dehydrogenase show the motions of the NAD^+ and NADH torsional angles X_n and X_{am}, as well as the puckering angle α_C for C4, are quite flexible as predicted by AM1 calculations. Molecular dynamics simulations with lobster D-glyceraldehyde 3-phosphate dehydrogenase, *L. casei* dihydrofolate reductase, and porcine heart malate dehydrogenase also show the puckering angle α_C for C4 of NADH to be quite flexible. With the various dehydrogenases the puckering motion of NADH is anisotropic, such that the C4 predominantly bends toward the substrate binding site. For each enzyme, steric hindrance by hydrophobic residues on the distal face of the cofactor are responsible for this anisotropic movement. In the dogfish lactate dehydrogenase pyruvate–NADH complex, the transferable pseudoaxial H_R at C4 comes within van der Waals contact with the carbonyl carbon of the substrate. Further, dynamics calculations indicate that the protonated imidazole group of HIS 193 is required not only as a general-acid catalyst but also for the correct alignment of pyruvate. The important catalytic features of the dogfish lactate dehydrogenase were examined by AM1 calculations using the X-ray coordinates for the enzyme around the active site and by molecular dynamics calculations using the entire enzyme. These features are the following: (i) in the ground state, approach of all reactants to within van der Waals radii; (ii) in the transition state, proton transfer from imidazolium cation (ImH_2^+) of HIS 193 to substrate carbonyl oxygen is almost complete while hydrogen transfer from 1,4-dihydronicotinamide to carbonyl carbon is about midway. The late transition state for proton transfer from ImH_2^+ is facilitated by the repulsive positive charges of ImH_2^+ and the arginine guanidinium cation substituent of ARG 106. It is proposed that the major driving forces in the catalysis are the steric compression in the ground state, the lateness of proton transfer which provides a large partial positive charge on the carbonyl carbon, and the preequilibrium puckering of the 1,4-dihydronicotinamide ring to *quasi*-boat conformation with transfer of the pseudoaxial hydrogen. The favoring of A- or B-side hydrogen transfer is determined by shielding of one side of the 1,4-dihydronicotinamide ring, which prevents access of substrate to and dynamic deformation at the unblocked side. An earlier proposal that dehydrogenases evolved in such a manner to level their dynamics by having NADH assume the weaker reductant *anti* antiperiplanar conformation (**1a**) in H_R transfer (A-side) and the stronger reductant *syn* antiperiplanar conformation (**1b**) in H_S transfer (B-side) cannot be correct on the basis of the AM1 potential energies of these conformations (i.e., **1a** and **1b** should be comparable reducing agents). In *L. casei* dihydrofolate reductase, the weakly polar interactions of oxygen functions of THR 45, ILE 13, and ALA 97 with the hydrogens of C2-H, C4-H, and C6-H of NADPH do not represent hydrogen bonds previously thought to be important in the activation of the cofactor. In the dehydrogenases in general, the amino acid oxygen functionalities which point inwards toward the nicotinamide ring are involved in hydrogen bonds to water molecules in the apoenzyme thereby keeping the cofactor binding site open.

Introduction

It has been appreciated for some time that in a given dehydrogenase, only one of the two prochiral hydrogens on C4 of the 1,4-dihydronicotinamide ring of NAD(P)H will be transferred in the reaction and this stereospecificity of transfer is usually absolute.[2] This gives rise to the A-specific and B-specific classes of dehydrogenases (Chart I). A-specific enzymes catalyze *pro-R* hydrogen removal from NAD(P)H {and *re* face addition of hydrogen to $NAD(P)^+$} and B-specific enzymes catalyze *pro-S* hydrogen removal from NAD(P)H {*si* face addition of hydrogen to $NAD(P)^+$}. In a recent review, You lists some 156 A-specific and 121 B-specific dehydrogenases.[2]

An early concept of merit for A and B stereospecificity simply involved the shielding of one side of the nicotinamide plane by the protein structure. Limited to this simplistic assumption, the A or B stereospecificity would seem to depend on chance.

(1) Contribution in partial satisfaction of the Ph.D. degree in chemistry.
(2) For a review on stereochemical aspects of NAD(P) dehydrogenases, see: You, K-s. *CRC Crit. Rev. Biochem.* **1984**, *17*, 313.

0002-7863/93/1515-2125$04.00/0

Chart I

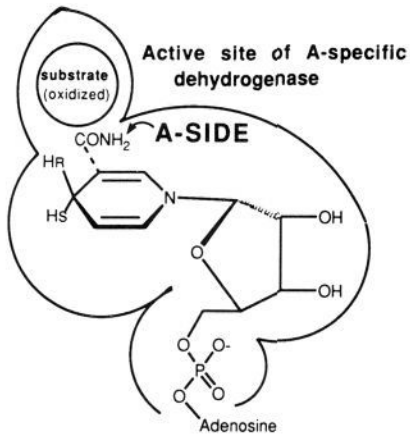

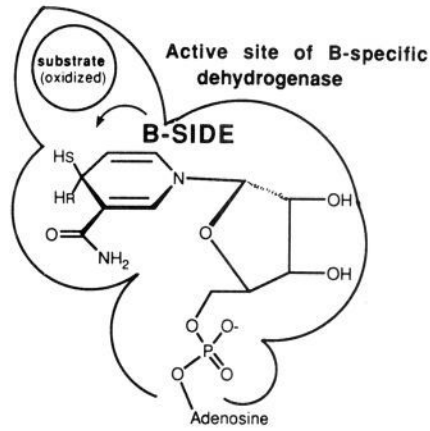

However, Benner offered a hypothesis for a rational requirement for A/B stereospecificity.[3] Benner observed a correlation between the stereospecificities of a number of dehydrogenases and the equilibrium constant for the enzymatic reaction (eq 1). Examination of 24 enzymes revealed that A-side (*pro-R*) dehydrogenases

$$\mathrm{R(HCOH)R' + NAD(P)^+ \overset{K_{eq}}{\rightleftharpoons} R(C{=}O)R' + NAD(P)H} \quad (1)$$

were those where $K_{eq} < 10^{-11.2}$ ($10^{-17.5}$ to $10^{-11.3}$), while B-side (*pro-S*) dehydrogenases were those where $K_{eq} > 10^{-11.2}$ ($10^{-11.1}$ to $10^{-7.5}$). It was stipulated that NAD(P)H exist at the active sites in the *anti* antiperiplanar conformation (**1a**) (Chart II) for A-side transfer and the *syn* antiperiplanar conformation (**1b**) for B-side transfer. Benner proposed the 1,4-dihydropyridine rings of **1a** and **1b** to be in *quasi*-boat conformations with the hydrogen to be transferred from C4 pseudoaxial. The association of A-side transfer with **1a** and B-side transfer with **1b** was proposed to have evolved to suitably match the energetics of the substrate–product redox couple. In order to do so, it is required that *anti* antiperiplanar NADH (**1a**) be a weaker reductant than *syn* antiperiplanar NADH (**1b**). In this treatment the *anti* periplanar (**1c**) and *syn* periplanar (**1d**) conformers are not considered to be of biological importance. However, the X-ray structure of glutathione reductase,[4] when taken with Benner's proposal of hydrogen transfer from a pseudoaxial position of a *quasi*-boat conformer for 1,4-dihydropyridine, requires the bound NADPH to be in the *anti* periplanar conformation **1c**. Further, ^{1}H NMR studies with type II dihydrofolate reductase[5] strongly implicate the **1d** conformation, since *pro-R* hydrogen is transferred from a distinct *syn* conformation. Oppenheimer, among others, has challenged Benner's hypothesis on the basis of some general considerations and several other exceptions.[6]

Using ab initio calculations, Houk and Wu employed *N*-(hydroxymethyl)-1,4-dihydropyridine (**2a**) and *N*-ethyl-1,4-dihydropyridine (**2b**) as models for NADH.[7] Their results indicate that, as seen in X-ray structures, the 1,4-dihydropyridine nucleus prefers a planar conformation, but that substitution at N induces some deformation toward a *quasi*-boat form for the ring. A hydroxymethyl substituent on N, perpendicular to the plane of the 1,4-dihydropyridine ring, results in the largest degree of the latters puckering. Hydride transfer from **2a** to methyliminium ion using the 6-31G* basis set indicated that the transition state for delivery of hydride antiperiplanar to the C–O bond is 1.4 kcal/mol lower in potential energy than when the cofactor has a periplanar transition state structure. This value is in agreement with an experimental value determined by Benner.[3a]

Chart II

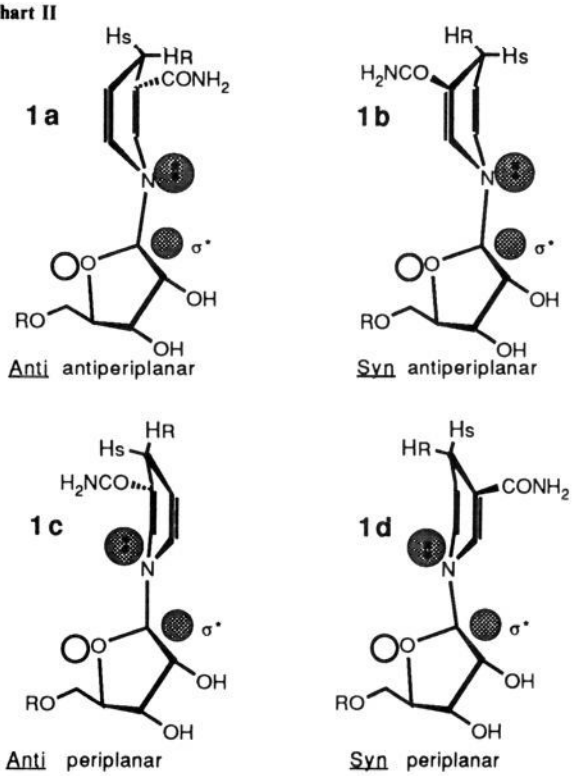

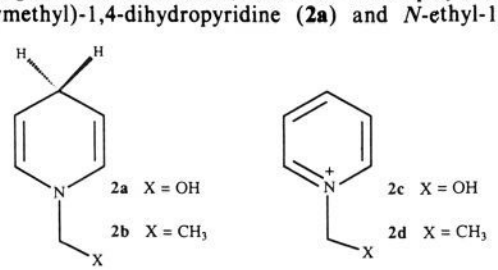

The present study employs AM1 semiempirical calculations and CHARM$_m$ molecular dynamics simulation experiments in the evaluation of the mechanism of NAD(P)H dehydrogenase enzymes using known structure of enzymes. AM1 calculations have been employed to evaluate the potential energies of the conformations of *N*-(1,β-ribosyl)-1,4-dihydronicotinamide (**3H**) and *N*-(1,β-ribosyl)nicotinamide (**3**) as defined by the torsion angles X_n, X_{am}, α_C, and α_N (Chart III). Reaction coordinate calculations were used to evaluate the kinetic significance of these conformational parameters. In disagreement with Benner's hy-

(3) (a) Benner, S. A. *Experentia* **1982**, *38*, 633. (b) Nambiar, K. P.; Stauffer, D. M.; Kolodzjiej, P. A.; Benner, S. A. *J. Am. Chem. Soc.* **1983**, *105*, 5886. (c) Benner, S. A. In *Mechanistic Principles of Enzymatic Activity*; Liebman, J. F., Greenberg, A., Eds.; VCH Publishers Inc.: New York, 1988; pp 56–59.

(4) Pai, E. F.; Karplus, P. A.; Schulz, G. E. *Biochemistry* **1988**, *27*, 4068.

(5) Brito, R. M. M.; Rudolph, F. B.; Rosevear, P. R. *Biochemistry* **1991**, *30*, 1461.

(6) Oppenheimer, N. J. *J. Am. Chem. Soc.* **1984**, *106*, 3032.

Chart III

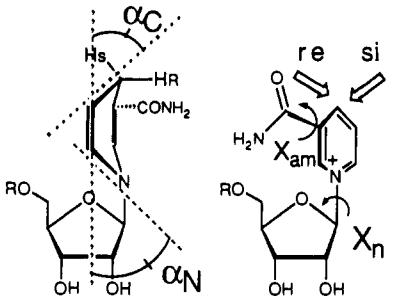

3H 3

pothesis, the very small differences in reduction potentials between conformers **1a** and **1b** could hardly match the range of equilibrium constants associated with eq 1. Also, it is shown that switching from antiperiplanar to periplanar (**1a,b** vs **1c,d**) does not provide a great difference in the facility of H^- transfer (loc. cit. and see ref 7). Supportive evidence has been derived for the aspect of Benner's hypothesis which holds that there is a kinetic advantage to having the 1,4-dihydronicotinamide ring boat shaped such that the hydrogen to be transferred is pseudoaxial. Sampling the conformations of *N*-(1,β-ribosyl)-1,4-dihydronicotinamide at the active sites of a number of dehydrogenases by molecular dynamics establishes an anisotropic bending of the planar 1,4-dihydropyridine ring to a *quasi*-boat conformation with the transferable hydrogen being directed toward the substrate site. In dogfish muscle lactate dehydrogenase pyruvate–NADH complex, H_R is in the pseudoaxial position and continuously in van der Waals contact with the substrate carbonyl carbon. The effect of the key active site residues, HIS 193 and ARG 106[8] in this enzyme, on the catalysis of hydride transfer has been considered by AM1 with models constructed from the X-ray coordinates from the Brookhaven Protein Databank.

Methods

The AM1 program[9] was implemented on a Silicon Graphics Iris 4D/220 workstation in the MOPAC 6.0 package (QCPE 455). Initial coordinates for **3** were obtained by adjustments of the X-ray structure of NAD^+–lithium salt[10] extracted from the Cambridge Structural Database[11] (CSD Refcode NADLIH10) using the molecular editor facility of Quanta 3.2 (Polygen-MSI corp.). All hydrogens were added and minimized with $CHARM_m$[12] v. 21.3 (Polygen-MSI) using the steepest descent algorithm, 100 steps, fixing the skeleton of the cofactor. The *N*-(β,1-ribosyl)-1,4-dihydronicotinamide (**3H**) was produced by adding a hydrogen at C4 of **3** and $CHARM_m$ minimizing the two hydrogens as before, fixing other parameters. Calculations were carried out with the standard AM1 program using the restricted Hartree–Fock (RHF) method. Geometries were optimized in internal coordinates and optimizations were terminated when SCF was attained, as determined by the satisfaction of Herberts test in the Broyden–Fletcher–Goldfarb–Shanno (BFGS) method.[13]

$CHARM_m$ molecular dynamics were run on the Silicon Graphics workstation and structural visualization and manipulation was performed in Quanta. The following coordinate files were extracted from the Brookhaven Database: (a) dogfish lactate dehydrogenase inhibitor complex with oxamate, entry **1LDM**,[14a] and apoenzyme, entry **6LDH**;[14b] (b) *L. casei* dihydrofolate reductase complex with methotrexate, entry **3DFR**;[14c] (c) porcine heart malate dehydrogenase, entry **4MDH**;[14d] and (d) lobster muscle glyceraldehyde 3-phosphate dehydrogenase, entry **1GPD**.[14e] The coordinates of the pdb file **1LDM**[14a] were modified as follows for dynamic studies: Only polar hydrogens were added to the enzyme structure, and extended atoms were used for all carbon chains. The $CHARM_m$ topology file AMINO.RTF was used for the enzyme residues. In the case of protonated HIS 193, a $CHARM_m$ residue HSC from the residue topology file was specified at this position, otherwise histidines were left unprotonated (residue HIS). Water molecules were treated as TIP3P residues.[15] The cofactor unit was modified to include all hydrogens and in addition C4 of the nicotinamide was modified so as to give both NADH and NAD^+. A $CHARM_m$ atom type CUA1 was used for carbons 2, 3, 5, and 6 of the 1,4-dihydronicotinamide of NADH and NP was used for the pyridine nitrogen. The parameter file PARM.PRM was modified to include the following angle parameters: (a) O–P–O = 112.0° (by inference from X-ray structures[14]); force constant 100 kcal/mol·Å, and (b) CUA1-NP-CUA1 = 117.2° (from the X-ray structure of *N*-methoxymethyl-1,4-dihydronicotinamide[16]); force constant 120 kcal/mol·Å. Partial charges for NADH and NAD^+ were obtained by AM1 calculation of both species (1SCF). Pyruvate was generated in the 2-D modeling facility Chemnote in Quanta, minimized, and superimposed on oxamate in the 3D modeling mode. The keto carbonyl was superimposed on the amide carbonyl and the carboxylates of oxamate and pyruvate were carefully overlapped. Assemblies of other enzymes with cofactors, and inhibitor in the case of dihydrofolate reductase 3DFR, were treated in the same manner. All assemblies were minimized prior to dynamics studies: 100 steps of steepest descents algorithm minimization with a force criterion of 0.001 kcal/10 steps were followed by the adopted basis Newton–Raphson algorithm for 2000 steps (tolerance 1×10^{-9} kcal/10 steps). Hydrogen bonds and nonbonding interactions were cut off at 5.0 and 14.0 Å, respectively, and were updated every 25 steps. Dynamics to 100 ps using a time step of 0.001 ps (1000 steps/ps) were run using Verlet integration. The following protocol was used: a heating phase of 3 ps to a final temperature of 300 K, followed by equilibration of 57 ps, and finally 40 ps of observation. Coordinates were printed every 0.05 ps, rendering 800 structures from the 40 ps of collection phase.

Table I. Heats of Formation[a] in AM1 for **3H** in Planar and Puckered Conformations

α_C[b]	α_N[b]	H_f	ΔH_f[c]
0	0	−191.7	
10	10	−190.0	1.72
20	20	−182.4	9.32
10	0	−190.7	0.98
15	5	−189.9	1.78

[a] Potential energy in kcal/mol. [b] See Chart III for definition. [c] Difference in heats of formation between puckered and planar ($\alpha_C = \alpha_N = 0$) conformations of **3H**.

Results

Conformational studies were carried out with **3** and **3H** (Chart III) using the AM1 semiempirical program with attention to (i) the nicotinamide deformation angles α_C and α_N, (ii) the torsion angle of the ribose C_1–N bond (X_n), and (iii) the rotation of the amide substituent (X_{am}). We will first discuss modification of the deformation angles α_C and α_N.

The Deformation Angles α_C and α_N and the Puckering of the 1,4-Dihydropyridine Ring (Chart III). Using the graphical pro-

(7) Wu, Y-D.; Houk, K. N. *J. Am. Chem. Soc.* **1991**, *113*, 2353.
(8) ARG 109 in *B. stearothermophilus* lactate dehydrogenase has been shown by mutagenesis to be very important to the mechanism: Clarke, A. R.; Wigley, D. B.; Chia, W. N.; Barstow, D.; Atkinson, T.; Holbrook, J. J. *Nature* **1986**, *324*, 699.
(9) Dewar, M. J. S.; Zoebisch, E. G.; Healy, E. F.; Stewart, J. J. P. *J. Am. Chem. Soc.* **1985**, *107*, 3902.
(10) Reddy, B. S.; Saenger, W.; Muhlegger, K.; Weimann, G. *J. Am. Chem. Soc.* **1981**, *103*, 907.
(11) Cambridge Structural Database (CSD), available from Medical Foundation of Buffalo, Inc., Research Institute, 73 High Street, Buffalo, NY 14203-1196.
(12) Brooks, B. R.; Bruccoleri, R. E.; Olafson, B. D.; States, D. J.; Swaminathan, S.; Karplus, M. *J. Comput. Chem.* **1983**, *4*, 187.
(13) Cioslowski, J.; Kertesz, M. *QCPE Bull.* **1987**, *7*, 159.
(14) The following X-ray structures were obtained from the Brookhaven database (July 1991 release, Brookhaven National Laboratory). (a) Dogfish lactate dehydrogenase ternary complex with oxamate, pdb file 1LDM: Abad-Zapatero, C.; Griffith, J. P.; Sussman, J. L.; Rossmann, M. G. *J. Mol. Biol.* **1987**, *198*, 445. (b) Dogfish lactate dehydrogenase apoenzyme, pdb file 6LDH: White, J. L.; Hackert, M. L.; Buehner, M.; Adams, M. J.; Ford, G. C.; Lentz, P. J., Jr.; Smiley, I. E.; Steindel, S. J.; Rossmann, M. G. *J. Mol. Biol.* **1976**, *102*, 759. (c) *L. casei* dihydrofolate reductase, pdb file 3DFR: Filman, D. J.; Bolin, J. T.; Matthews, D. A.; Kraut, J. *J. Biol. Chem.* **1982**, *257*, 13663. (d) Porcine heart malate dehydrogenase, pdb file 4MDH: Birktoft, J. J.; Rhodes, G.; Banascak, L. J. *Biochemistry* **1989**, *28*, 6065. (e) Lobster glyceraldehyde 3-phosphate dehydrogenase, pdb file 1GPD: Moras, D.; Olsen, K. W.; Sabesan, M. N.; Buehner, M.; Ford, G. C.; Rossmann, M. G. *J. Biol. Chem.* **1975**, *250*, 9137.
(15) Jorgensen, W. L.; Chandrasekar, J.; Madura, J. D. *J. Phys. Chem.* **1983**, *79*, 926.

Table II. Selected Structural Parameters for NAD(P)(H) Cofactors in Protein Data Bank Entries of Dehydrogenase Enzymes

PDB code[a,b]	resolution[c]	X_{am}[d,e]	X_n[d,f]	α_C[d,g]	α_N[d,h]
4mdh (NAD+)*	2.5	161.7	-95.8	0.4	1.1
11dm (NADH)*	2.1	173.6	-106.0	7.3	6.0
21db (NADH)	3.0	-175.3	-123.5	5.7	9.9
51dh (NADH)	2.7	170.0	-86.8	1.5	10.4
31dh (NADH)	3.0	-177.3	-139.5	7.2	6.0
7dfr (NADPH)	2.5	168.8	-110.6	3.8	8.2
8dfr (NADPH)	1.7	-179.8	-109.1	2.5	8.1
3dfr (NADPH)*	1.7	-175.6	-122.6	8.0	6.9
6adh (NAD+)	2.9	-149.6	-103.6	3.2	3.7
1gpd (NAD+)*	2.9	-179.9	45.3	0.9	0.7
3gpd (NAD+)	3.5	152.6	66.4	3.6	2.4

[a] Four-letter codes in filenames pdbxxxx.ent. For journal references to structures marked with an asterisk, see footnote 14. [b] Bound cofactor in brackets. [c] In units of Å. [d] Defined in Chart III. [e] X_n is the O1–C1(ribose)–N–C2(nitotinamide) torsion angle in degrees. [f] X_{am} is the O(amide)=C–C3–C2 torsion angle in degrees. [g] Angle in degrees between C4 and the mean plane of C2, C3, C5, and C6 on the nicotinamide ring. [h] Angle in degrees between N1 and the mean plane of C2, C3, C5, and C6 on the nicotinamide ring.

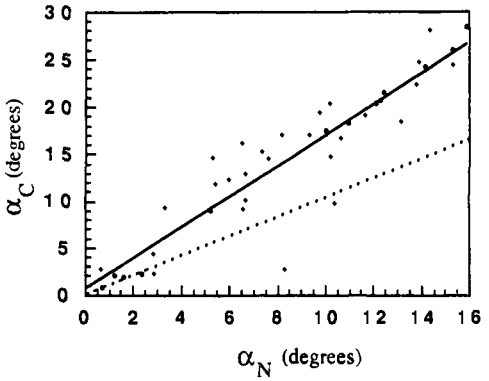

Figure 1. A plot of deformation angles α_C vs α_N from the X-ray structures for 1,4-dihydropyridines found in the Cambridge Crystallographic Database (α_C and α_N defined in Chart III): solid line, least-squares fit of all datapoints (see eq 2); dashed line, $\alpha_C = \alpha_N$.

gram Quanta and its molecular editor, the planar structure for **3H** (with $X_n = -80°$ and $X_{am} = 170°$, the latter as seen in the X-ray structure of dogfish muscle lactate dehydrogenase[14a]) was brought into *quasi*-boat form, care being taken to leave bond lengths unchanged. After the positions of carbon and nitrogen atoms of the nicotinamide ring were fixed, all other parameters were optimized and the heats of formation were calculated using AM1 (Table I). It is noteworthy, that puckering such that $\alpha_N = \alpha_C = 10°$ involves only 1.7 kcal/mol destabilization of the structure in AM1. However, when $\alpha_N = \alpha_C = 20°$ the heat of formation is increased to 9.3 kcal/mol with respect to the flat ground state geometry. It requires only 1 kcal/mol to deform the 1,4-dihydronicotinamide to $\alpha_C = 10°$ when $\alpha_N = 0°$ and, finally, $\alpha_C = 15°$, with a modest $\alpha_N = 5°$ demands 1.8 kcal/mol. Table II contains values for α_C observed from X-ray structures of enzyme bound NAD(P)H as registered in the Brookhaven database for comparison.

Glasfeld et al. have summarized α_C and α_N values for *N*-alkyl-1,4-dihydronicotinamides archived in the Cambridge Structural Database.[16] In general, the deviations are very small, on the order of 1–2°. Extending the search to all 1,4-dihydropyridines found in the Cambridge Structural Database, α_C is almost always larger than α_N, suggesting that pyramidalization at N1 is impeded relative to puckering at C4.[17] The linear plot (eq 2 and Figure

$$\alpha_C = 1.64(\alpha_N) + 0.63 \quad (2)$$

(16) Glasfeld, A.; Zbinden, P.; Dobler, M.; Benner, S. A.; Dunitz, J. D. *J. Am. Chem. Soc.* **1988**, *110*, 5152.

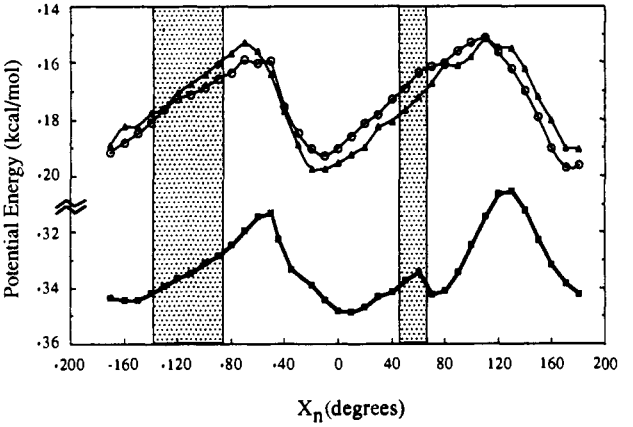

Figure 2. Calculated heats of formation in AM1 for **3** with nicotinamide ring conformation (a) *planar* (squares), (b) *deformed toward the re face* (circles); and (c) *deformed toward the si face* (triangles). X_{am} is *trans* to C2 as in the Brookhaven database. Deformation angles of $\alpha_C = 15°$ and $\alpha_N = 5°$ were used for both. Shaded areas represent the observed range of values of X_n in dehydrogenase structures in the Brookhaven databank (see Table II).

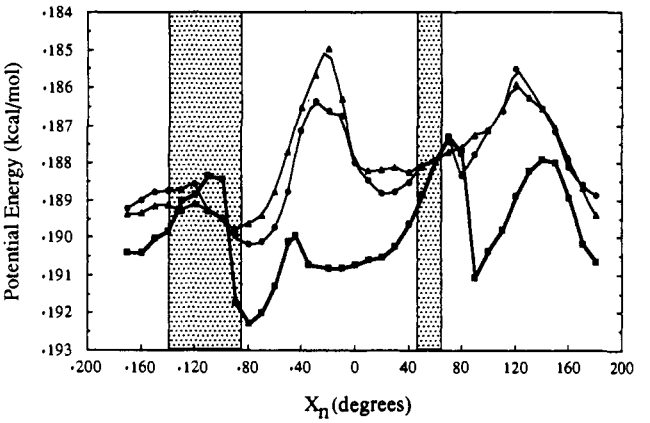

Figure 3. Calculated heats of formation in AM1 for **3H** vs X_n with 1,4-dihydronicotinamide ring conformation (a) *planar* (squares), (b) *deformed to place pro-R pseudoaxial* (circles), and (c) *deformed to place pro-S pseudoaxial* (triangles). X_{am} is *trans* to C2 as in the Brookhaven database. Deformation angles of $\alpha_C = 15°$ and $\alpha_N = 5°$ were used for both. Shaded areas represent the observed range of values of X_n in dehydrogenase structures in the Brookhaven databank (see Table II).

1) of α_C vs α_N is associated with a modestly good correlation factor of $r = 0.92$. The slope of ~1.64 is significant, whereas the intercept of 0.63, which would indicate that at $\alpha_N = 0$ the value of $\alpha_C = 0.63°$, is perhaps questionable. Maximum puckering is associated with highly substituted structures and a maximal α_C value of 28° is seen with a 1,4-dihydro Hantzch ester.

Deformation of the oxidized nicotinamide 3 is found to be much more energetically costly. Thus, AM1 calculations with $\alpha_C = \alpha_N = 10°$ and $\alpha_C = 15°$ with $\alpha_N = 5°$ both entail raising the ground state by 15 ± 1 kcal/mol relative to the flat conformation for the pyridine ring. Any mechanism in which the pyridine ring of **3**

(17) Cambridge crystallographic references for Table III: (a) Freeman, G. R.; Bugg, C. E. *Acta Crystallogr., Sect. B* **1974**, *30*, 431. (b) Voet, D. *J. Am. Chem. Soc.* **1973**, *95*, 3763. (c) Inoue, M.; Sakaki, T.; Fujiwara, T.; Tomita, K. *Bull. Chem. Soc. Jpn.* **1978**, *51*, 1118. (d) Koyama, H. *Z. Kristallogr.* **1963**, *118*, 51. (e) Karle, I. L. *Acta Crystallogr.* **1961**, *14*, 497. (f) Ishitani, O.; Yanagida, S.; Takamuku, S.; Pac, C. *J. Org. Chem.* **1987**, *52*, 2790. The following structure files (listed by Cambridge refcode) were used in the construction of Figure 1: BELGUU, BELHAB, BELHEF, BELHIJ, BELHUV, BETKIU, BICCAR, BICCEV, BICCIZ, BICCOF, DEVFIT, DIDZOF, DOTTOV, DUGPAW, DUWBIG, EXCMHP, FANNAJ, FIJFAF, FIJFEJ, FIPTUT, FIPVAB, FULNIJ, FULNOP, GICHUV, JEHLUD, JENHIT, MACPHF, MECHPY, MPECXP, PRHNCA01, SACYOK, TAGBEI, TAGBIM, BDHNIC, FIXCUK, FIXDAR, PRHNCA.

is in *quasi*-boat conformation with $\alpha_C + \alpha_N = 20°$ requires the latter to be a steady state intermediate.

The torsion angle X_n (Schematic I) was varied in increments

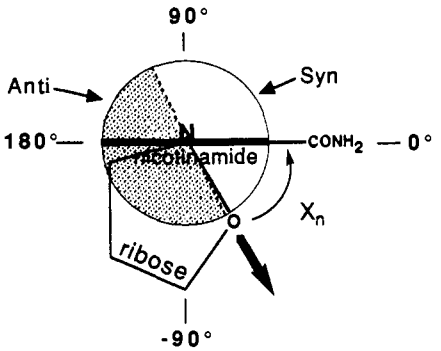

Schematic 1

of 10°, with $\alpha_N = \alpha_C = 0°$ and $X_{am} = 170°$, and heats of formation were calculated in AM1, with SCF optimization of all parameters except X_n. The results for **3** (Figure 2) and **3H** (Figure 3) show that the energetically preferred values of X_n for **3** (+10°) and **3H** (−80°) are quite different. The energy minimum of X_n for **3** corresponds to a *syn* conformation, whereas the minimum for **3H** dictates an *anti* conformation (see Schematic I). The barriers for rotation away from the energy minima of X_n for **3** and **3H** are 4 and 4 to 5 kcal/mol, respectively. Local minima of X_n for **3H** (X_n = 40 and 180°) are of ~2 kcal/mol greater potential energy than the global minima. For **3**, the *syn* energy minimum (X_n = 10°) exists at an insignificantly 0.5 kcal/mol below an *anti* minimum (X_n = −170°).

Inspection of the Protein Data Bank entries for NAD(P)H and NAD(P)$^+$ complexes of dehydrogenases shows that the values for X_n vary between −87° and −140° for the A-specific enzymes (nine structures). These values correspond (Table II) to the cofactor bound in the *anti* conformations (as in **1a** and **1c**). There are only two entries for B-specific enzymes and for these the cofactor is bound in the *syn* conformations (as in **1b** and **1d**) with X_n values of 45° and 66°. The latter two entries represent glyceraldehyde 3-phosphate dehydrogenases.[18] The X_n values of NAD(P)H conformations found in A-specific and B-specific enzymes are included as the two shaded areas in the plot of potential energy vs X_n (Figures 2 and 3) generated by AM1 calculations using **3** and **3H**.

Plots of potential energy vs X_n when $\alpha_C = 15°$ and $\alpha_N = 5°$ for **3** and **3H** are included in Figures 2 and 3, respectively. Deformation of both structures to *quasi*-boat forms was produced in directions of both *re* and *si* faces of the nicotinamide ring (for **3**) and with *pro-R* and *pro-S* alternately pseudoaxial (for **3H**). For **3**, X_n is at minimal potential energy in the *anti* conformation (X_n = 170°), although, as in the case of $\alpha_C = \alpha_N = 0$, the difference between *syn* (X_n = 10°) and *anti* conformations is less than 1 kcal/mol. The *syn* minima (X_n = −10° for *re* deformation and X_n = −20° for *si* deformation) are slightly shifted relative to the flat conformer (X_n = 10°). When **3** is restricted to the range of allowed X_n values in the dehydrogenase enzymes (shaded areas in Figures 2 and 3) the potential energies of the *quasi*-boat conformation are independent of X_n. Plots of potential energy vs X_n for **3H** differ depending upon values of α_C and α_N; however, the minimum at X_n = −80° is retained. For enzyme bound NAD(P)H potential energies are marginally higher than at the minimum X_n value of −80° for the flat 1,4-dihydronicotinamide in **3H**.

The dependence of X_n upon X_{am} was investigated. The potential energy as a function of X_n for **3** and **3H** at X_{am} = 0° was determined and compared to those calculated when X_{am} = 170°. The results (not shown) indicate that for both **3** and **3H**, the potential energy of X_n has a small dependence, ~1 kcal/mol, on X_{am}. However, the positions of X_n minima are very similar when

(18) See ref 14e and pdb file *pdb3gpd.ent*: D-glyceraldehyde 3-phosphate dehydrogenase from human muscle, by H. C. Watson and J. C. Cambell (1983) and references therein.

Chart IV

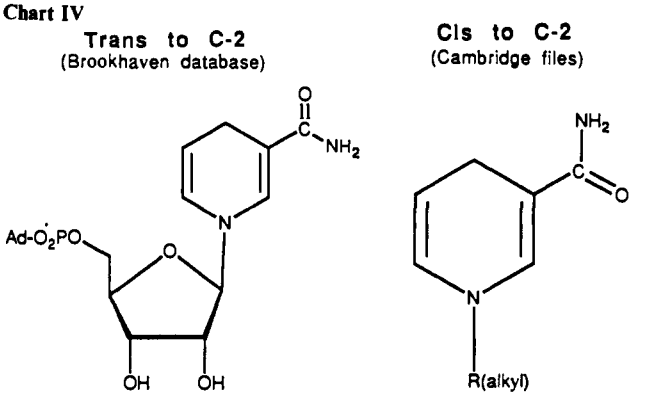

Table III. Selected Structural Parameters for *N*-Alkyl Nicotinamides and 1,4-Dihydronicotinamides in the Cambridge Structural Database

Refcode[a]	X_{am}[b]	X_n[c]	author(s); year
MNICPC	4.6	n.a.	Freeman et al.; 1974[17a]
NICADN	−3.1	n.a.	Voet; 1973[17b]
MNICAC	152.0	n.a.	Freeman et al.; 1974[17a]
MNICAI	−166.6	n.a.	Freeman et al.; 1974[17a]
NADLIH10	−9.2	−165.4 (O)	Reddy et al.; 1981[10]
IACNCA	29.3	n.a.	Inoue; 1978[17c]
GICHUV	6.6	102.1 (O)	Glasfeld et al.; 1988[16]
PRHNCA01	21.0	100.2 (C)	Glasfeld et al.; 1988[16]
PRHNCA	−22.4	−101.3 (C)	Koyama; 1963[17d]
BDHNIC	3.8	−86.7 (C)	Karle; 1961[17e]
FIXCUK[d]	−166.1	94.5 (C)	Ishitani; 1987[17f]
FIXDAR[e] (A)	−14.0	61.1 (C)	Ishitani; 1987[17f]
FIXDAR (B)	15.8	−64.0 (C)	

[a] Cambridge Structural Database filename. [b] See **3** in Chart III. [c] Where applicable, β–Cα–N–C2 torsion angle. The identity of the β-atom on the N substituent is denoted in parentheses. [d] Oxidized nicotinamide ring. [e] 1,4-Dihydronicotinamide. A and B in the last entry refer to two distinct molecules in the asymmetric unit.

X_{am} = 0 (*cis* conformation, see Chart IV) or 180° (*trans* conformation).

The Torsional Angle X_{am} (Schematic II). Comparison of the

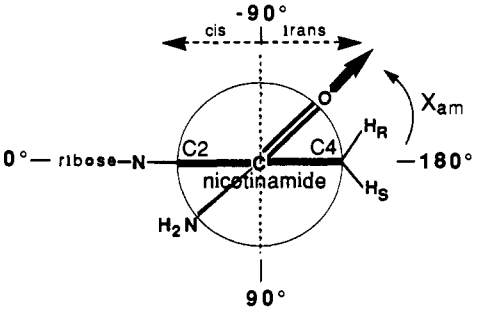

Schematic 2

X-ray structure of NAD$^+$, nicotinamides, and 1,4-dihydronicotinamides (Cambridge file, see Table III[17]) to those of enzyme bound NAD$^+$ and NADH (Brookhaven database) shows that when free, the amide O is *cis* to C2 (X_{am} ~ 0°, Chart IV and Schematic II), whereas in X-ray structures of NAD$^+$ bound to enzymes the O is *trans* to C2 (X_{am} ~ 180°, Chart IV and Schematic II), whereas in X-ray structures of NAD$^+$ bound to enzymes the O is *trans* to C2 (X_{am} ~ 180°, Chart IV and Schematic II). The AM1 heats of formation when amide O is *trans* (X_{am} = 170°) are consistently higher than when *cis* (X_{am} = 0°) such that the amide being cis to C2 is the global minimum arrangement.[19]

Shown in Figure 4 is the dependence of the AM1 potential energies of **3** and **3H** on X_{am} [X_n = −80° for **3H** and 10° for **3** (see Figures 2 and 3)]. In practice, the optimizations of all other parameters were carried out at values of X_{am} that were varied in

(19) Cummins, P. L.; Gready, J. E. *J. Mol. Struct. (THEOCHEM)* **1989**, *183*, 161.

Chart V

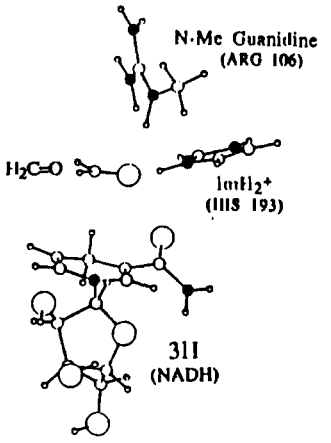

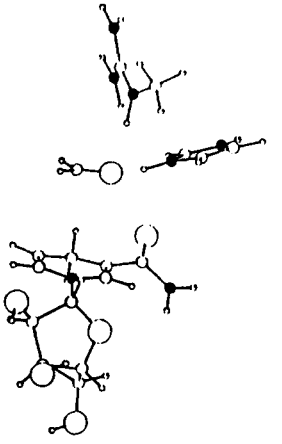

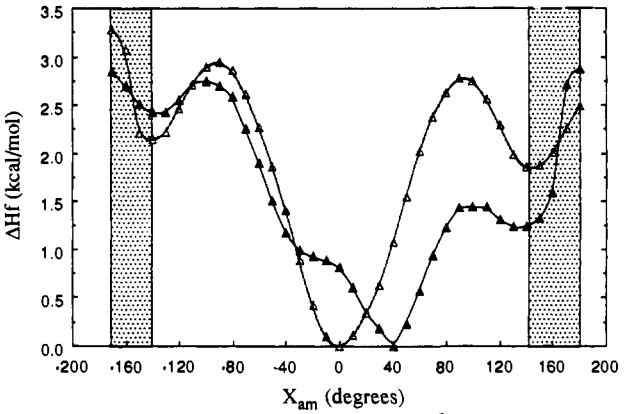

Figure 4. Calculated heats of formation in AM1 for **3** (solid triangles) and **3H** (open triangles) vs X_{am} in degrees relative to minimum energy conformation (X_n = −80° for **3H** and +10° for **3** and $\alpha_C = \alpha_N = 0°$). Shaded areas represent the observed range of values of X_{am} in dehydrogenase structures in the Brookhaven databank (see also Table II).

increments of 10°. Three minima exist for **3H**. The global minimum at X_{am} = 0° corresponds to a conformation in which the amide group and the pyridine ring are coplanar with the ring C2 and the amide oxygen *cis*, affording an extended π-system formed between the amide function and the 1,4-dihydropyridine ring. Two local minima at −150° and 150° involve the amide carbonyl being coplanar to the *pro-R* and *pro-S* hydrogens, respectively (Schematic II). On the AM1 level, the local minima have potential energies about 2 kcal/mol higher than the global minima. For **3**, the global minimum occurs at X_{am} = 40° which also corresponds to a *cis* arrangement of the ring C2 and the amide carbonyl oxygen. Planarity is not required with the electron-deficient pyridine ring. Two local minima are observed at −140° and 140°. These are 1 and 2.3 kcal/mol, respectively, above the global minimum of **3**. The barriers to rotation of the amide functional group are approximately 3 and 1.5–2.7 kcal/mol for **3H** and **3**, respectively.

The importance of catalytic amino acid residues in the dehydrogenase reaction was investigated by use of the spacing of formaldehyde, **3H**, and functional groups (Chart V) as seen in the X-ray structure of dogfish muscle lactate dehydrogenase reported by Rossmann and co-workers (Brookhaven datafile **1LDM**[14a]). For the construction of Chart V the C2, C3, C5, and C6 atoms of the pyridine ring of **3H** were superimposed on the corresponding positions of the pyridine ring of enzyme bound nicotinamide (α_C and α_N of **3H** were both 0°) and the formaldehyde substrate was placed by superimposition of its carbonyl on pseudosubstrate oxamate amide carbonyl while protonated imidazole (ImH_2^+) was placed by superimposition on the imidazole function of HIS 193. Methylguanidine was superimposed on the side chain of ARG 106.

With use of all functionalities shown in Chart V, a reaction trajectory for H^- transfer was mapped with no constraint on the position of the proton on ImH_2^+. The transition state of lowest calculated potential energy is associated with a very late transition state for proton transfer from ImH_2^+ to carbonyl oxygen while the transfer of hydride is midway. The AM1 potential energy for this transition state is 31 kcal/mol above the starting state and the enthalpy of reaction is 4 kcal/mol. An early transition state for proton transfer was also calculated with protonated guanidine and with ImH_2^+ intact. The transition state is raised by 10 kcal/mol by AM1, compared to the transition state with almost full transfer of the proton. The AM1 calculation dictates that the proton be more or less fully transferred to the substrate in the transition state.

The AM1 calculations with the functionality from the X-ray structure of lactate dehydrogenase may be viewed as being, at least partially, in the solution phase. As a means of certain comparisons with quantum calculations carried out by others, we have investigated several systems which are essentially in the gas phase. In the first instance, a proton is placed 1.10 Å from the carbonyl oxygen of the substrate formaldehyde (eq 3). The relative

$$\mathbf{3H} + H_2CO\text{–}H^+ \rightarrow \mathbf{3} + H_3COH \qquad (3)$$

spacing of substrate and cofactor is still as in Chart V. The calculated enthalpy of activation for this reaction is 27 kcal/mol and the reaction is exothermic by 24 kcal/mol. Formation of the AM1 transition state is accompanied by the proton located on the formaldehyde oxygen entering into a hydrogen bond with the dihydronicotinamide amide carbonyl oxygen (**4**). This hydrogen

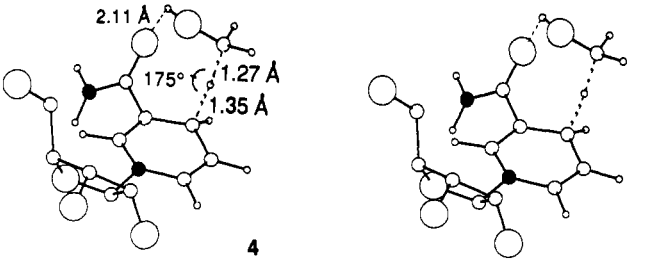

4

bond serves to tether the substrate intimately to the hydride donor and results in a transition state structure which is marked by an 8-membered ring through $\overline{C_4\cdots H\cdots C{=}O\text{–}H\cdots O{=}C\text{–}C_3}$. If the amide carbonyl oxygen in the reaction of eq 3 is *cis* to C2 of the pyridine ring the transition state is destabilized by more than 10 kcal/mol. This is in accord with the observations of Cummins and Gready, who have carried out AM1 calculations in the modeling of dihydrofolate reductase.[20]

In the uncatalyzed reaction, the substrate is left unprotonated (eq 4) and **3H** is in the **1a** conformation with the amide oxygen

$$\mathbf{3H} + H_2CO \rightarrow \mathbf{3} + H_3CO^- \qquad (4)$$

(20) Cummins, P. L.; Gready, J. E. *J. Comput. Chem.* **1990**, *11*, 791.

Chart VI

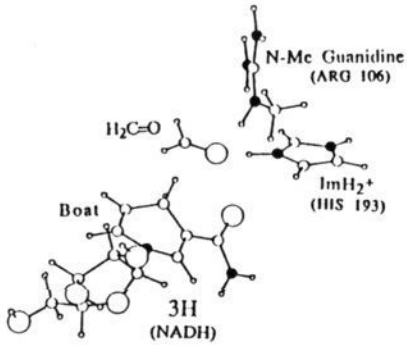

cis to C2 (it is *trans* in the enzymatic reaction, loc. cit.). As the transition state structure is formed the amide has moved out of plane to allow the $-NH_2$ to hydrogen bond with the developing negative charge on the oxygen of the putative methoxide. The transition state structure was found to be 61 kcal/mol above the starting structure and the overall reaction is endothermic by 50 kcal/mol. As expected for a very endothermic reaction, the transition state for hydride transfer is very late. These large enthalpy values indicate that in the absence of acid catalysis, the reaction does not proceed ($k \approx 10^{-32}$ M^{-1} s^{-1}).

The Kinetic Importance of the Torsional Angle X_n. In the previous calculations of reaction trajectories X_n was allowed to adjust from the minimal value for **3H** (−80°) to the minimal value for **3** (10°) so that the potential energy remained at a minimum as the reaction of eq 3 proceeded along the reaction coordinate. We find that maintenance of the X_n at −80° throughout the reaction trajectory calculations provides essentially no change in AM1 activation enthalpies. Thus, the values of X_n are not of much significance in determining the activation energy.

The Kinetic Importance of *Anti* Antiperiplanar (1a) vs *Anti* Periplanar (1c) Conformations. In the preceding experiments the relative positions of the ribose ring oxygen and H_R of **3H** have been as in **1a** (antiperiplanar) and H_R was transferred. An AM1 comparison of the reaction of eq 3 using the **3H** in **1c** (periplanar) conformation with H_S transfer showed that **1a** is favored by 1.2 kcal/mol, when $\alpha_C = 15°$ and $\alpha_N = 5°$ was considered. Furthermore, calculations with $\alpha_C = 15°$ and $\alpha_N = 5°$ show that transfer of H_S, when pseudoaxial in a **1b** conformation of **3H**, is within 1 kcal/mol of the activation energy for pseudoaxial H_R transfer (**1a**). Therefore, there is no appreciable stereoelectric preference for any one of the conformations **1a**–**1d** that could be used to explain A/B-side preference for hydride transfer in the dehydrogenase enzymes.

The Kinetic Importance of 1,4-Dihydronicotinamide Ring Puckering. As shown via AM1 calculations, bending the planar 1,4-dihydronicotinamide toward a boat conformation requires little expenditure of energy if the sum of the deformations (α_C and α_N) is no greater than about 20°. This puckering places a C4-hydrogen in a pseudoaxial position (Chart VI). The three-dimensional structure of Chart V was employed in the construction of Chart VI. The location of the 2, 3, 5, and 6 carbons of the puckered ($\alpha_C = \alpha_N = 10°$) 1,4-dihydropyridine correspond to like carbon atoms of the pyridine ring in Chart V. The reaction involves a concerted H^+ transfer from ImH_2^+, which is late, and transfer of the pseudoaxial H_R. AM1 calculations provide an activation enthalpy of 22 kcal/mol which is 5 kcal/mol lower than the value calculated for the same reaction with a planar 1,4-dihydropyridine ring. The decrease in transition state energy may be attributed to the increase in driving force for hydride expulsion due to an increased p-character at the C4–H_R bond allowing greater orbital overlap throughout the trajectory (Chart VII). Since the bent 1,4-dihydropyridine ring with $\alpha_C = \alpha_N = 10°$ resides 1.7 kcal/mol above the planar structure, the kinetic advantage of this *quasi*-boat structure is a bit above 3 kcal/mol, provided the differences in potential energies are reflected in free energies of activation. Calculations involving other values of α_C and α_N in reactions with the reactants of Chart VI are considered. A mere 1 kcal/mol is

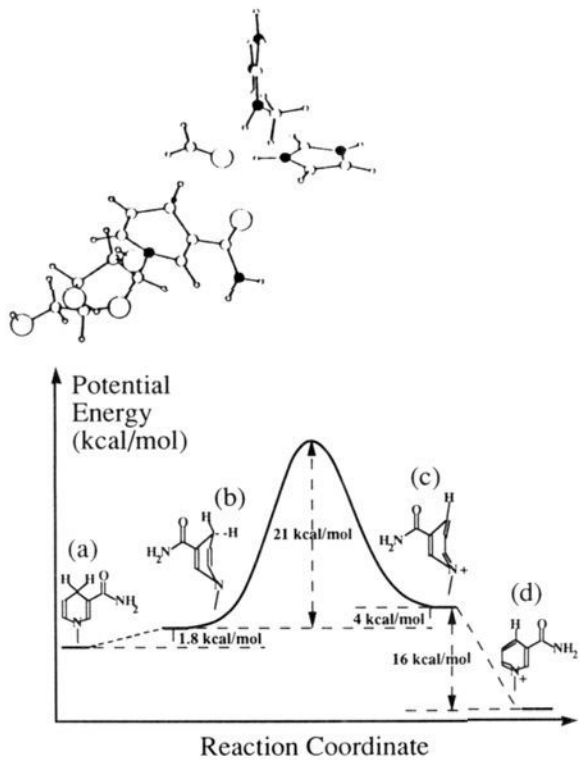

Figure 5. Reaction coordinate for the reduction of H_2CO by **3H** in the presence of protonated methylguanidine and protonated imidazole. The reactants were arranged as in the X-ray structure of dogfish muscle lactate dehydrogenase (ref 14a, Chart V), containing NADH, pseudo-substrate oxamate, the imidazole of HIS 193, and the guanidine of ARG 106. (a) 1,4-Dihydronicotinamide moiety in a planar conformation, (b) 1,4-dihydronicotinamide moiety in a puckered conformation ($\alpha_C = 15°$ and $\alpha_N = 5°$), (c) nicotinamide moiety in a puckered conformation ($\alpha_C = 15°$ and $\alpha_N = 5°$), and (d) nicotinamide moiety in a planar conformation.

Chart VII

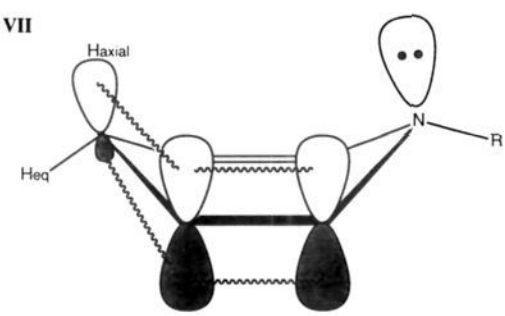

required to form a "half-boat" conformation of **3H** with $\alpha_C = 10°$ and $\alpha_N = 0°$ and the transition state structure was found to be 24 kcal/mol above the "half-boat conformation" of the starting structure. This is comparable (25 kcal/mol) to the potential energy necessary to form the transition state from flat **3H** when a bent structure of $\alpha_C = \alpha_N = 10°$ is intermediate. Finally, with $\alpha_C = 15°$ and $\alpha_N = 5°$ an activation enthalpy of 21 kcal/mol is obtained for attainment of the transition state while promoting the ground state to the deformed 1,4-dihydronicotinamide requires 1.8 kcal/mol.

Due to resonance stabilization, it is anticipated that bending of the pyridine ring of a nicotinamide should be much more difficult than the bending of a 1,4-dihydronicotinamide. In the retrograde direction of the imidazole general-base catalyzed oxidation of CH_3OH by **3**, the puckered conformation of **3** ($\alpha_C = \alpha_N = 10°$) resides 15 kcal/mol above the planar conformation such that the ground state of **3H** + $CH_2O{\cdots}HImH^+$ and the immediate product state of **3** + $CH_3OH{\cdots}ImH$ are of comparable

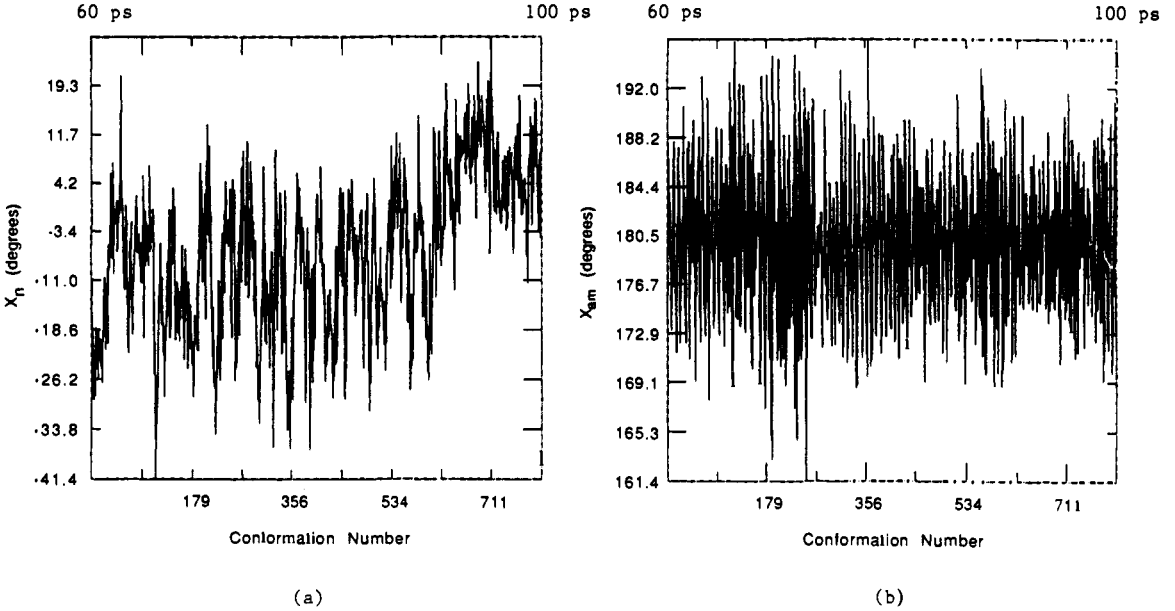

Figure 6. Molecular dynamics simulations of NAD^+ in dogfish muscle lactate dehydrogenase: (a) the change in X_n with time (ps) and (b) the change in X_{am} with time (ps).

Chart VIII

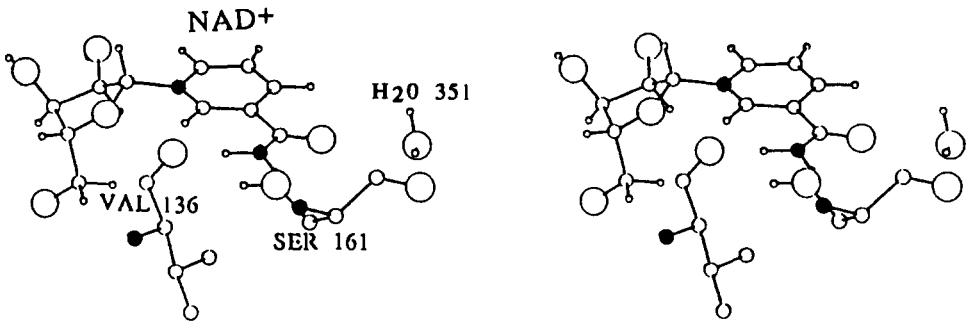

potential energy (Figure 5). In fact, the reaction is calculated to be slightly endothermic, but it can be viewed as an equilibrium process. This represents the favored reaction trajectory for the dehydrogenase enzyme according to AM1.

Molecular dynamics simulation of dehydrogenases in apoenzymes, holoenzymes, and ternary complex forms were carried out to 100 ps at 300 K using a number of dehydrogenase structures from X-ray coordinates deposited in the Brookhaven files.[14] A detailed study was performed with lactate dehydrogenase from dogfish muscle[14a] whose X-ray structure contains NADH, oxamate pseudosubstrate, and three water molecules at the active site. In the structure, Oγ of the THR 245 side chain and O (carbonyl) of VAL 136 are within van der Waals distance to H5 and H2 of NADH, respectively. A structure, sans oxamate pseudosubstrate, with NAD^+ plus the three water molecules was created by computer modification of the X-ray structure. Dynamic studies on the enzyme have been carried out with (a) $NAD^+ + 3H_2O$ at the active site with the ImH of HIS 193 unprotonated and substrate absent, (b) $NADH + 3H_2O$ at the active site with the ImH of HIS 193 protonated with pyruvate present, (c) $NADH + 3H_2O$ at the active site with the ImH of HIS 193 unprotonated with pyruvate present, and (d) apoenzyme[14b] alone. With the other dehydrogenase enzymes, only NADH was used and substrates/inhibitors absent, except for the case of dihydrofolate reductase[14c] (see Methods). NAD(P)H was superimposed on the position of the cofactor molecule in the X-ray structures of (e) *L. casei* dihydrofolate reductase (NADPH),[14c] (f) porcine heart malate dehydrogenase (NADH),[14d] and (g) lobster muscle glyceraldehyde 3-phosphate dehydrogenase (NADH).[14e]

(a) Dogfish Muscle Enzyme with $NAD^+ + 3H_2O$ at the Active Site with the ImH of HIS 193 Unprotonated and Substrate Absent. X_n and X_{am} were mapped as a function of trajectory in the collection phase of MD. These torsional angles show considerable flexibility (Figure 6a,b). Especially interesting is the variation of X_n, which oscillates with an average value of 0° {sweep of 65° from −41° to 27°} corresponding to an *anti* conformation of ribose with respect to the nicotinamide ring (as in **1a**). X_{am} values oscillate between the local minimum positions at ±150° (determined here by AM1 and by others[19]). In dogfish muscle lactate dehydrogenase, the amide side chain of NAD^+ is held by hydrogen bonding to the hydroxyl of SER 161, the carbonyl O of VAL 136, and water molecule 351 (Chart VIII) such that it is not free to rotate over to the minimum position of 0° which is optimal for NAD^+. In the enzyme, the range of angles observed for X_{am} varies from 127° to 196° (Figure 6b).

(b) Dogfish Muscle Enzyme with $NADH + 3H_2O$ at the Active Site with the ImH of HIS 193 Protonated and Pyruvate Substrate Present. Pyruvate substrate replaced oxamate of the X-ray structure by a superimposition of carboxylate groups with the substrate keto oxygen oriented toward the NH^+ proton of HIS 193 (Chart IX). Initial coordinates and partial charges for pyruvate were obtained by AM1 calculations. The results of the MD simulation (Figure 7a,b) show that X_n varies in time between −155° and −109°, the range being smaller than that observed for NAD^+ in the absence of substrate (compare Figures 6a and 7a). The values again correspond to an *anti* conformation of ribose and nicotinamide rings (**1a**) and are consistent with the AM1 calculated preference for out-of-plane arrangement of the ribose ring C–O bond to the nicotinamide ring of NADH (Figure 3). X_{am} values fall between 150° and 204° (a *trans* conformation) such that the –C=O of the amide moiety rotates considerably to both sides of the NADH plane.

The oxygen of the $-CONH_2$ remains adjacent to the proton on HIS 193 throughout the MD calculations. This interaction

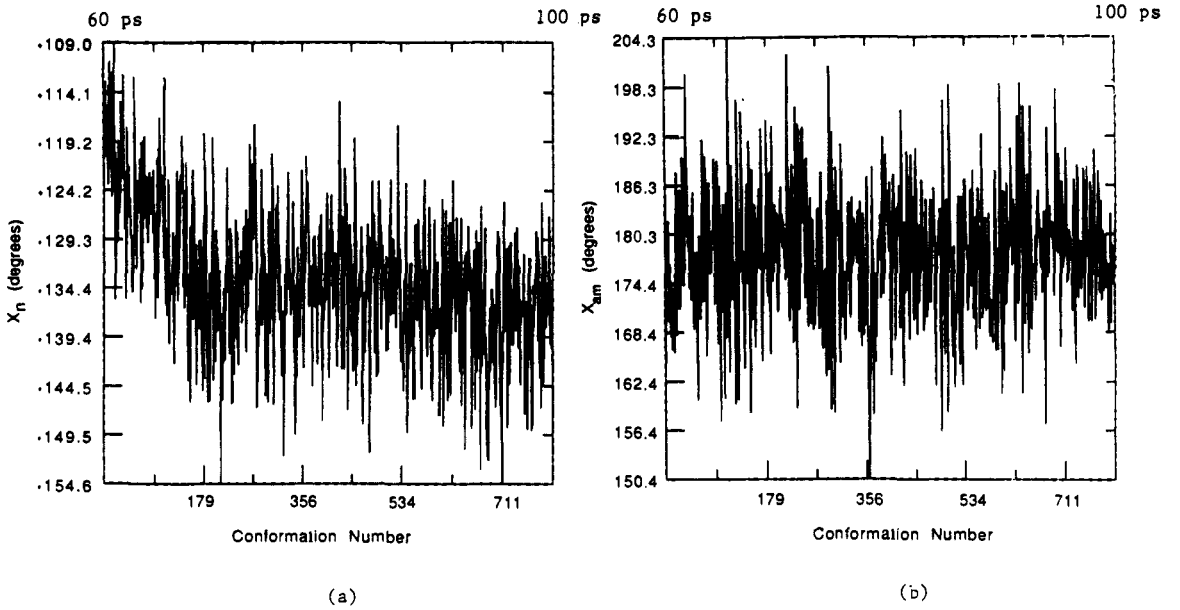

Figure 7. Molecular dynamics simulations of NADH in dogfish muscle lactate dehydrogenase substrate complex (ES): (a) the change in X_n with time (ps) and (b) the change in X_{am} with time (ps). The ES complex was constituted by replacing the oxamate of the X-ray structure with pyruvate and protonating the catalytic imidazole of HIS 193.

Chart IX

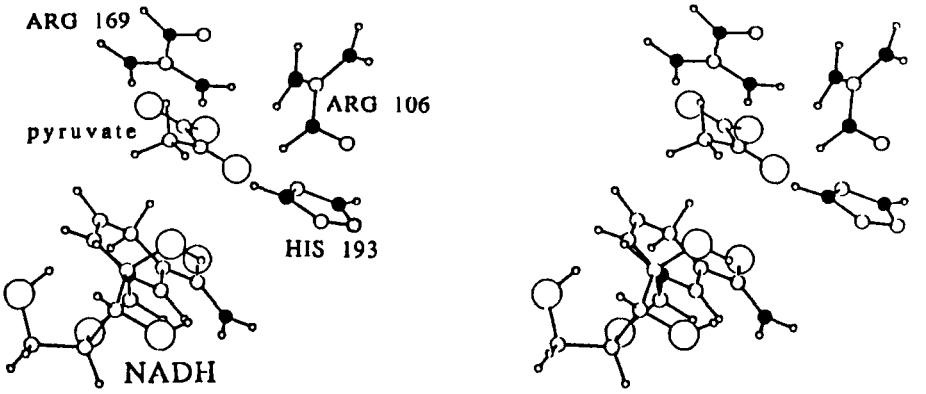

Chart X

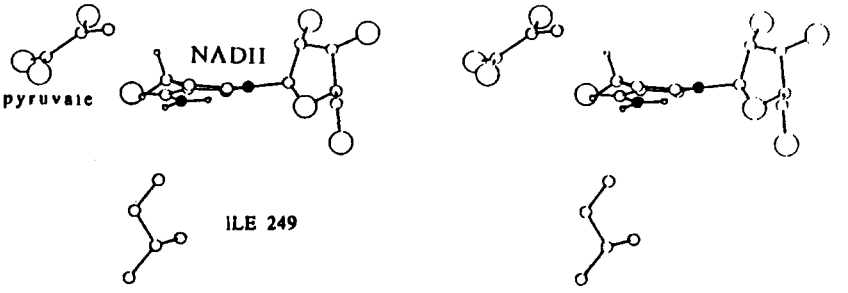

can only be a small stabilizing factor in a ground state, since the distance is usually on the order of 2.5 Å and the oxygen is underneath the plane of the imidazolium ion such that any hydrogen bond would have to be at ~90°. ARG 106 is above the substrate and distal to the cofactor with a guanido NH within hydrogen bonding distance to the keto carbonyl oxygen of pyruvate. This situation remains throughout the MD calculation. Other interactions of the substrate with the enzyme and cofactor found to be very stable over the 40 ps sampling time include a salt bridge between the carboxylate and ARG 169 and a hydrogen bond between the carbonyl oxygen of the keto function and the imidazolium ion of HIS 193.

To follow changes of α_C and α_N during the course of MD, we have monitored two improper dihedral angles. The virtual angle between the vectors C2–C6 and C4–C3 was used to evaluate α_C and the angle between the vectors C3–C5 and N1–C6 was used to evaluate α_N. Figure 8 shows a distribution plot of calculated α_C angles during conformation sampling. Of the 800 structures collected over 40 ps, 97.6% (781) of the structures pucker toward a boat conformation in a fashion which directs the pseudoaxial H_R (A-side hydrogen) toward the pyruvate carbonyl carbon, 0.4% of the time (3 structures) the ring structures are exactly planar, and the remaining 2% (16 structures) are puckered away from the substrate. A bulky isoleucine side chain (ILE 249) on the B-face of the cofactor is mainly responsible for the anisotropic movement of C4 (Chart X and Table IV).

The distance between the pseudoaxial A-side hydrogen of NADH and the keto carbonyl carbon was mapped as a function of time during MD as shown in Figure 9. A distribution curve is observed where the average distance is 2.7 Å. This is approximately the sum of van der Waals radii for the two nuclei and, therefore, attractive forces within the complex of cofactor

Chart XI

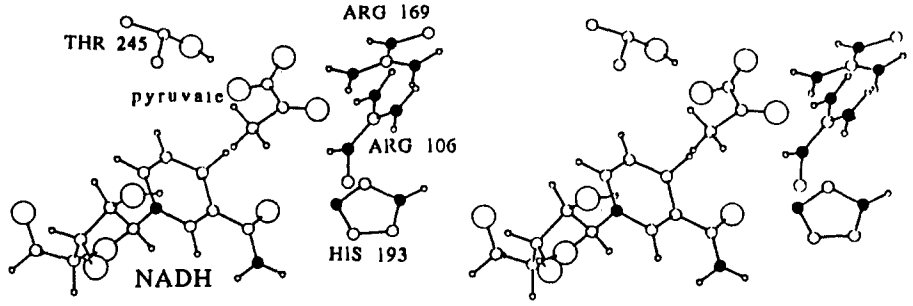

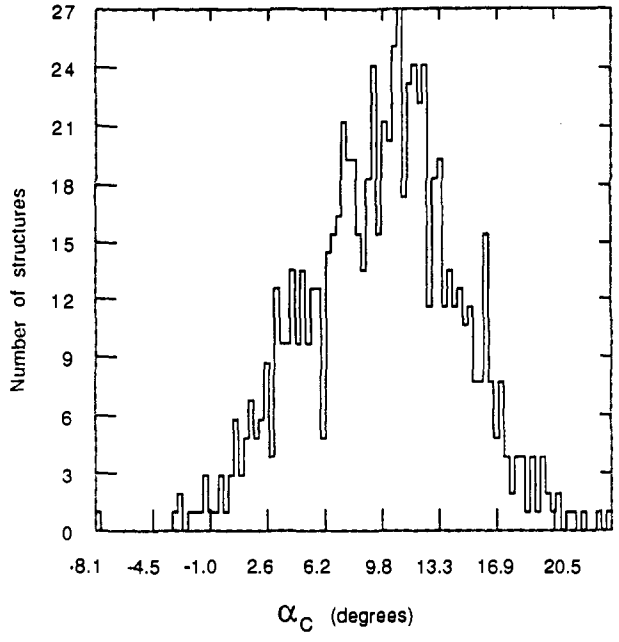

Figure 8. Molecular dynamic simulations of NADH in dogfish muscle lactate dehydrogenase. Distribution of α_C deformation angles in the simulation with pyruvate bound and the imidazole protonated on HIS 193.

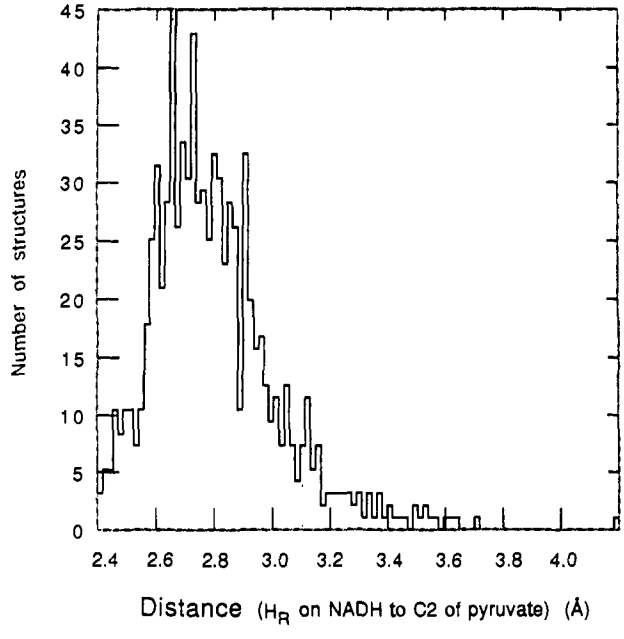

Figure 9. Molecular dynamics simulations of NADH in dogfish muscle lactate dehydrogenase. Distribution curve of H_R to C(=O){pyruvate} distances. Pyruvate is bound and the enzyme is protonated on HIS 193.

Table IV. Average Deformation Angles α_C and α_N[a] for 1,4-Dihydronicotinamide Rings of NAD(P)H in CHARM$_m$ Molecular Dynamics Simulations of Dehydrogenases and Identities of Amino Acid Residues Distal to the Substrate Site in the Nicotinamide Binding Pockets

	α_C[b]	α_N[b]	distal residue(s)[c]
lactate dehydrogenase (1LDM)[14a]	10	8	ILE 249, VAL 136
dihydrofolate reductase (3DFR)[14c]	6	3	PHE 103
malate dehydrogenase (4MDH)[14d]	4	8	ALA 245, LEU 157
glyceraldehyde 3-P dehydrogenase (1GPD)[12e]	3	5	ILE 12, TYR 317

[a] In degrees. [b] See Chart III for definition. [c] Nonpolar amino acid residue side chain in the nicotinamide binding pocket responsible for anisotropic puckering of the 1,4-dihydronicotinamide ring.

and substrate are optimized. The reactants within the ground state complex are thus poised to enter the transition state for hydride transfer.

In our computations with malate dehydrogenase holoenzyme[14d] and the dihydrofolate reductase holoenzyme inhibitor complex,[14c] the catalytic imidazole was not protonated. The extent of anisotropic motion of the C4 carbon for the dehydrogenases is compared in the plots of α_C vs α_N of Figure 10. From Figure 10, the primary motion of dihydronicotinamide C4 is in the direction of the substrate binding pocket. The order of anisotropic discrimination is dogfish muscle lactate dehydrogenase (97%) > porcine heart malate dehydrogenase (87%) > *L. casei* dihydrofolate reductase (85%) > lobster muscle glyceraldehyde 3-phosphate dehydrogenase (69%). Each enzyme contains a bulky hydrophobic substituent (LEU, ILE, or VAL) which provides steric hindrance to the movement of the nicotinamide C4. Glyceraldehyde 3-phosphate dehydrogenase shows only a modest preference for puckering toward the B-face of the 1,4-dihydronicotinamide ring of NADH. It may be argued that the mechanism of this enzyme is so different from those of the three other dehydrogenases used that it probably cannot be compared.[21] Table IV summarizes the average values for α_C and α_N for each enzyme, as well as the identity of the residue(s) which hinder the motion of C4 of each nicotinamide binding pocket.

(c) Dogfish Muscle Enzyme with NADH + 3H$_2$O at the Active Site with the ImH of HIS 193 Unprotonated and Pyruvate Present. Aside from acting as general-acid catalyst, protonated HIS 193 is essential for the correct arrangement of the substrate. On removing the proton from HIS 193, the torsion angle X_{am} undergoes a marked shift in range from 150–204° to 134–189°. This amounts to the average disposition of the C=O of the –CONH$_2$ group from being on the side of the pyridine ring facing the substrate to being on the distal side of the pyridine ring (Chart XI). Without a proton on HIS 193, the angle X_n, during the dynamics for the enzyme substrate complex, was observed to be between –89° and –45° as compared to X_n = –155° to –109° when protonated. This change in X_n results from steric hindrance between the carboxamide substituent of NADH and the nonprotonated HIS 193. The distance between the imidazole ring nitrogen and carboxamide oxygen becomes 4 Å on average. The most dramatic changes involve substrate binding. In the absence of protonation, HIS 193 can no longer anchor the pyruvate keto

(21) See: Liu, L.; Huskey, W. P. *Biochemistry* **1992**, *31*, 6898 and references therein.

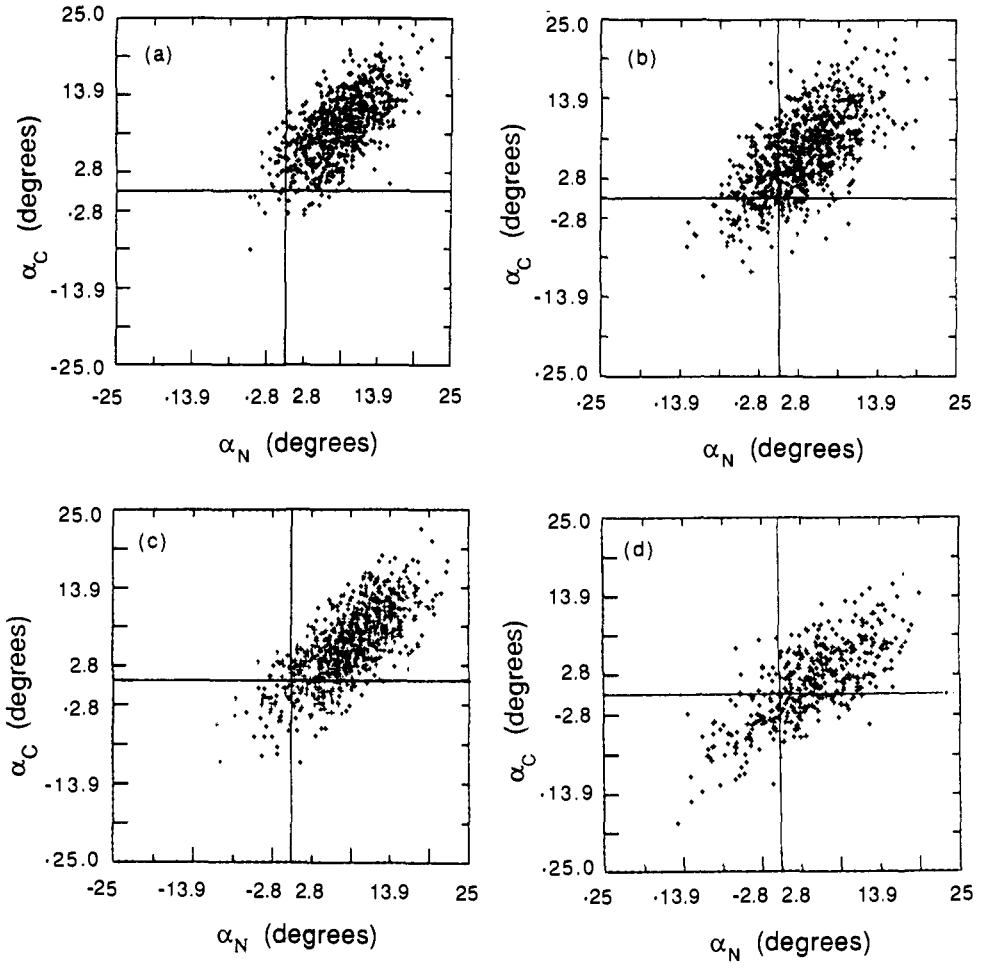

Figure 10. Molecular dynamics simulations of NAD(P)H in dehydrogenases. Plots of α_C vs α_N (defined in **3H**) during collection phases of MD (40 ps): (a) dogfish muscle lactate dehydrogenase,[14a] (b) *L. casei* dihydrofolate reductase,[14c] (c) porcine heart malate dehydrogenase,[14d] and (d) lobster muscle D-glyceraldehyde 3-phosphate dehydrogenase.[14e] Examination of plots a–d shows the dissymmetry of motion of C4–H toward the substrate.

Chart XII

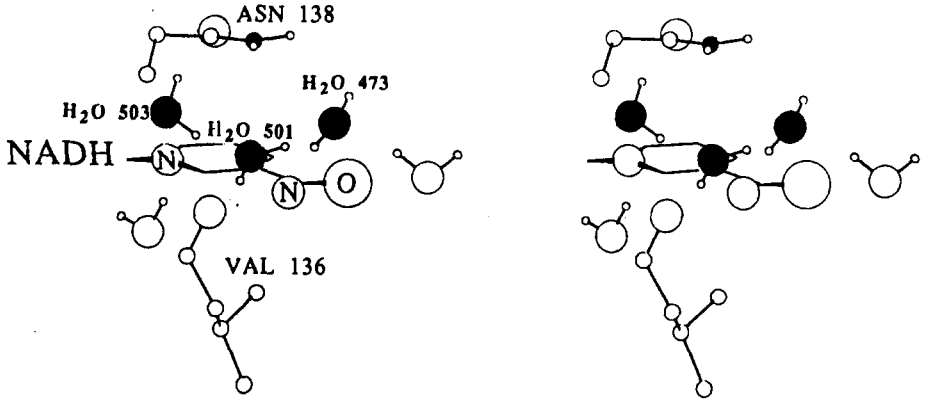

carbonyl, and for this reason the average structure from MD has the substrate rotated away from the cofactor and engaged in a reinforced hydrogen bond with the guanidinium ion of ARG 106 (Chart XI). The pyruvate carboxylate has rotated to shift the oxygen atom which was *syn* to the keto carbonyl over to the distal nitrogen of ARG 169. The bifurcated hydrogen bond of the salt bridge between ARG 169 and the substrate carboxylate has been reduced to a single hydrogen bond. A short hydrogen bond has formed between the hydroxyl on the side chain of THR 245 and pyruvate carboxylate. The effect of this drastic conformational change is to increase the distance between the keto carbonyl and A-side hydrogen from 2.7 Å, when the imidazole ring is protonated, to an average distance of 3.9 Å. At no time during the 40 ps collection phase of MD does this distance become smaller than 3.0 Å. These features may be appreciated by inspection of Chart XI. Examination of the chart shows that the nonproductive ES complex formed in the absence of protonation of HIS 193 still contains the structural information for A-side hydrogen transfer. Thus, by MD the H_R of NADH becomes pseudoaxial 95% of the time (762 out of 800 structures).

(d) The Role of Water Which Occupies the NADH Binding Site of Dogfish Muscle Apolactate Dehydrogenase. The X-ray structure of the apolactate dehydrogenase[14b] shows that the cofactor site is occupied by 19 waters. Comparison of structures of enzyme and apoenzyme shows that NADH binding releases all but three of these water molecules: H_2O 553 associates with GLY 162 in the apoenzyme and corresponds to water 351 which associates with the carboxamide of NADH in enzyme, while H_2O molecules 359 and 492 occupy the substrate binding site of the enzyme. In the crystal structure of apoenzyme, three of the 19 water molecules

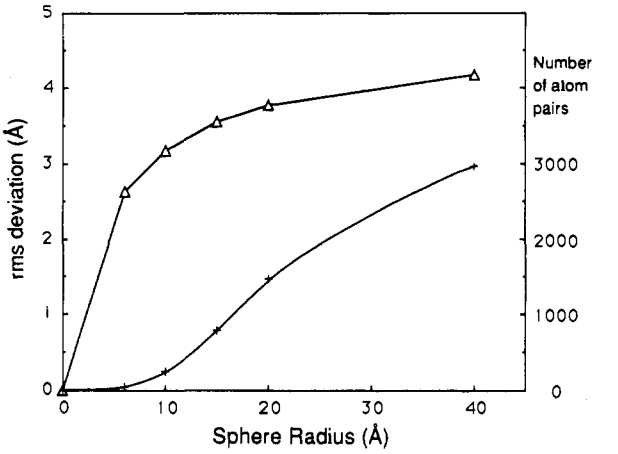

Figure 11. Molecular dynamics simulation of apolactate dehydrogenase from dogfish, when water molecules in the X-ray structure are excluded. Plots of (a) the calculated rms deviation in atomic positions (Å) between average MD structure and X-ray structure of apolactate dehydrogenase from dogfish muscle[14b] (triangles) and (b) the number of atoms which may be compared (crosses) as a function of sphere radius around active site HIS 193 (δ N).

(473, 501, and 503, each hydrogen bonded to the next) roughly occupy the positions of NH_2(amide), C3, and N1 of the nicotinamide moiety, respectively (Chart XII). This can be appreciated by careful superimposition of the X-ray structures of apoenzyme and enzyme.[22] Water 473 is hydrogen bonded to the carbonyl of VAL 136. The hydroxyl proton of SER 161 interacts with water molecule 474. The water molecules 473, 501, and 503, among others, maintain the protein geometry at the active site in the absence of cofactor. The amino acids associated with these water molecules {SER 161, VAL 136, and GLY 162} become associated with the nicotinamide ring. No remarkable changes occur during MD simulation of the hydrated enzyme. However, removal of the water molecules from within the active site of the apoenzyme and subsequent dynamic simulation reveals that (i) the opening where the pyrophosphate of NADH resides closes up due to movement of the side chain of ARG 198 into the space previously occupied by water molecules and (ii) ILE 249 comes up into the space where water molecules 473, 501, and 503 were located, compressing the site for the nicotinamide. This was ascertained by careful superimposition of the X-ray coordinates for the nicotinamide ring from the ternary complex structure.[14a] The vast changes at the active site as a result of dehydration can also be appreciated by analysis of the rms deviation of an average MD generated structure from the X-ray structure as a function of distance from the active site. The center of the active site was chosen as the δ nitrogen atom of HIS 193. Like atoms were matched and rms deviations between X-ray and average structures from MD were calculated for those pairs that occurred within a sphere of different sizes between 6 and 40 Å in radius. Since the approximate dimensions of the enzyme are 63 × 50 × 50 Å^3 and a 40 Å radius sphere encompasses all atom pairs (2970), a 6 Å sphere only contains essential features of the active site (53 atom pairs). According to Figure 11, rms deviation is, for the most part, derived from changes in the active site. In fact, over 75% of all change in atom positions occurs within a sphere of 10 Å radius. By this analysis, and comparison with the dynamic simulation where the water network is present, it is apparent that preservation of the active site pocket by hydrogen bonding of given functional groups to water, in the absence of cofactor, is an essential requirement for lactate dehydrogenase. The importance of the association of water molecules with amino acid functionalities will be considered in the Discussion section.

(22) Care should be exercised, since substantial changes occur upon substrate binding (see ref 14b). For a review on interaction of enzyme with cofactors, see: Grau, U. M. In *The Pyridine Nucleotide Coenzymes*; Everse, J., Anderson, B., You, K-s., Eds.; Academic Press: New York, 1982; pp 172–187.

Discussion

Quantum mechanical (AM1) and molecular dynamics (CHARMm MD) calculations combined with the X-ray structures of NADH dehydrogenase enzymes have been used to determine the following: (i) the potential energies of conformations of *N*-(β,1-ribosyl)nicotinamide (**3**) and *N*-(β,1-ribosyl)-1,4-dihydronicotinamide (**3H**) as determined by the deformation angles α_C and α_N and torsion angles X_n and X_{am}; (ii) the relationship of cofactor conformation to A-side and B-side specificity of dehydrogenase enzymes; (iii) the influence of conformations on the potential energy of activation for hydride transfer from C4 of **3H**; and (iv) the optimum mechanism for lactate dehydrogenase. We have evaluated Benner's hypothesis that kinetic advantages are to be had for *anti* antiperiplanar (**1a**) and *syn* antiperiplanar (**1b**) conformations of NAD(P)H and that there is also a kinetic advantage to the deformation of the nicotinamide ring to *quasi*-boat or *quasi*-semi-boat forms. All calculations have been carried out by use of the geometries at active sites as provided by X-ray structures deposited in the Brookhaven database (1991). These are as follows: from the laboratory of M. G. Rossmann, dogfish muscle lactate dehydrogenase (1LDM)[14a] and the corresponding apoenzyme (6LDH)[14b] as well as lobster D-glyceraldehyde 3-phosphate dehydrogenase (1GPD),[14c] from the laboratory of J. Kraut, *Lactobacillus casei* dihydrofolate reductase (3DFR),[14c] and from Birktoft et al. porcine heart malate dehydrogenase (4MDH).[14d]

We first address the question as to whether there is a kinetic advantage to the deformation of the nicotinamide ring to *quasi*-boat or *quasi*-semi-boat forms. The reader should refer to structures **1a–d**, **3**, and **3H** in the Introduction. AM1 calculations show that deformation of a planar 1,4-dihydronicotinamide (**3H**) toward a boat conformation with α_N and α_C = 10° requires 1.7 kcal/mol but the resultant potential energy for hydride transfer is decreased by 5 kcal/mol. If α_N = 5° and α_C = 15° the conformation change costs 1.8 kcal/mol but the activation enthalpy is decreased by 6 kcal/mol. Most importantly, molecular dynamics simulations with four NAD(P)H dependent dehydrogenase enzymes establish that an anisotropic puckering (Figure 10) to an average value of α_C = 5.5° (Figure 8 and Table IV) occurs such that the hydrogen to be transferred becomes pseudoaxial and approaches the carbon atom target to a van der Waals contact distance (Figure 9). In solution, the 1,4-dihydronicotinamide, not experiencing the effect of the enzyme environment, displays ring puckering, such that H_R and H_S become alternately pseudoaxial. The bottom of the nicotinamide pocket of the dogfish enzyme is comprised of hydrophobic residue side chains, an isobutyl group from ILE 249, and the isopropyl side chain of VAL 136. These hydrophobic groups cover the B-face of the nicotinamide ring and induce the anisotropic puckering motion by steric interactions with C4–H_S. We propose that an anisotropic ring deformation, placing the hydrogen to be transferred in an energetically favorable pseudoaxial position (Chart XI), is an essential feature of the mechanisms of these dehydrogenase enzymes (Figure 5b).

The conformational investigations in AM1 on *N*-β,1-ribosylated nicotinamide (**3**) and *N*-β,1-ribosylated 1,4-dihydronicotinamide (**3H**) show that the energy barriers for rotation of ribose around the nicotinamide (Schematic I) by systematically varying X_n (see Chart III) amount to about 4 kcal/mol (Figures 2 and **3**). The optimal X_n angles for **3H** place the C–O bond of the ribose ring perpendicular to the 1,4-dihydronicotinamide ring whereas the optimal X_n for **3** places the C–O bond nearly parallel to the nicotinamide ring.[23] The conformation of minimal energy (Figure

(23) These results agree with extrapolations of ab initio calculations using *N*-(hydroxymethyl)- and *N*-ethylnicotinamides by Houk and Wu (see ref 7). A shortcoming of the approach revolves around the use of *N*-(hydroxymethyl)-1,4-dihydronicotinamide to evaluate the torsion angle of N–C1–O5 and *N*-ethyl-1,4-dihydronicotinamide to separately evaluate the torsion angle of N–C1–C2 (where the ribose ring atoms are C1, C2, C3, C4, O5). In practice they obtain the same torsion angle for both in the case of the 1,4-dihydropyridines. It is clear from the results that this approach cannot differentiate between the positions for C2 and O5. The procedure does not allow the determination of the potential energy dependence of X_n when the N substituent is ribofuranose.

Chart XIII

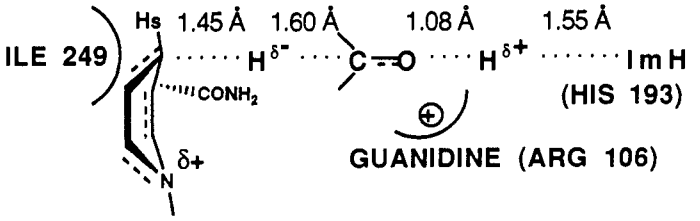

3) for **3H** is associated with an X_n value of −80° which corresponds to a *anti* conformation (**1a**, **1c**). The most favored X_n value for **3** (Figure 2) is at 10° which dictates a *syn* conformation (**1b**, **1d**).

The calculations alluded to in the previous paragraph were carried out with the torsion angle (X_{am}) for rotation of the nicotinamide amide bond set at 170° such that the amide oxygen is *trans* to C2 of the nicotinamide ring. The *trans* conformation is generally observed in X-ray structures of nicotinamide adenine nucleotides bound to dehydrogenases in both reduced and oxidized states. With the X_{am} value set to the minimal energy conformation of 0° for the non-enzyme bound NAD(P)H cofactor, the AM1 calculations with **3** and **3H** show that the values of X_n and X_{am} are not mutually dependent (data not shown).

Raber calculated by 3-21G* basis set that puckering of the aromatic ring of pyridine to a *quasi*-boat form with $\alpha_C = \alpha_N = 10°$ is minimally three times more energy demanding than the same deformation of 1,4-dihydropyridine.[24] We find by AM1 calculations that the same deformation of the 1,4-dihydronicotinamide **3H** requires 1.7 kcal/mol while the same deformation of nicotinamide **3** incurs 15 kcal/mol. This difference of ~13 kcal/mol is more than that required to explain the difference in binding propensities for NADH and NAD^+.[25] The apoenzymes have the lesser affinity for NAD^+, even though NAD^+ is present in the dogfish enzyme in a stable conformation with respect to X_n. The 100- to 1000-fold differences in dissociation constants[26] cannot be explained in terms of the conformational preferences for X_n. Examination of the reaction coordinate of Figure 5 reveals that the differences in potential energies to deform NADH and NAD^+ are such that the ground state potential energies for reactant {*quasi*-boat **3H** + $H_2CO\cdots HImH^+$} and immediate product {*quasi*-boat **3** + $CH_3OH\cdots ImH$} are of comparable potential energies. Further, X-ray data for a variety of 1,4-dihydropyridines show that C4 in general is more displaced out of the plane of the ring than the nitrogen (Figure 1). Very recently, Deng et al.[27] investigated the resonance Raman spectra of NADH specifically deuterated at the 4-position on the 1,4-dihydronicotinamide ring. The large observed changes in line positions for C–D bond stretch modes with C4–D_S (and comparatively small changes for C4–D_R lines) upon binding of the cofactor to lactate dehydrogenase and malate dehydrogenase were rationalized in terms of a *quasi*-boat conformation of NADH, which is consistent with a large deformation at C4. Vibrational analysis in semiempirical MO calculations further supported this view.

Molecular dynamics simulation studies on reduced and oxidized coenzyme in dogfish lactate dehydrogenase (Figures 6a and 7a) show that there is considerable flexibility of the X_n parameter such that it can adjust to approach a conformation which represents an energy minimum for unbound cofactor species. Also, AM1 reaction trajectories establish that the activation potential energy for hydride transfer from C4 of **3H** has little dependence upon X_n. There appears to be little kinetic advantage in the apoenzymes' preference for binding both NADH and NAD^+ with ribose C–O in the perpendicular conformation with respect to the nicotinamide rings. Benner's hypothesis[3] of considerable kinetic advantage to having the C–O bond of the ribose ring antiperiplanar to the nicotinamide plane seems to neglect dynamic behavior of the cofactor molecule, even when it is enzyme bound (see Introduction). Paramount to the hypothesis was the concept that **1a** is a much weaker reductant than **1b**. For the hypothesis to hold, the difference in potential energy for the two conformations must be on the order of 14 kcal/mol or more. Stereoelectronic arguments were presented to rationalize the difference between **1a** and **1b**, but inspection of the structures reveals that no great difference in stereoelectronic effect should exist between them. Indeed, quantum calculations employed here and elsewhere do not indicate any large differences between the two conformations. Thus, the difference in potential energy between **1a** and **1b** is approximately 2 kcal/mol in AM1.

The potential energy changes upon varying torsion angle X_{am} between the pyridine ring and the amide functional group {Schematic II} were reinvestigated by AM1 (Figure 4). In the enzyme bound nicotinamide cofactor, the amide oxygen and C2 of the pyridine ring are *trans*. In the case of dogfish muscle lactate dehydrogenase the *trans* conformation is apparently held by hydrogen bonds between the amide C=O and OH of SER 161 and the amide NH with the C=O of VAL 136. In an AM1 examination of the reaction of 1-methyl-1,4-dihydronicotinamide with pyrazine, Gready and Cummins found that a hydrogen bond could form between the amide carbonyl oxygen in the *trans* conformation and the protonated substrate.[20] This feature brings the reactants together to form a complex. The possibility for such a role by the amide carbonyl oxygen in *trans* conformation in enzymatic reactions was considered by Gready and Cummins. We believe that such interaction is of little significance. For dogfish lactate dehydrogenase, the only possible hydrogen bonding between amide carbonyl and substrate would involve the lactate hydroxyl group and the amide of NAD^+. Presumably, however, the hydroxyl proton of lactate is involved in hydrogen bonding to the general-base imidazole group of HIS 193. In another study it was proposed[28] that the amide carbonyl oxygen is out of plane and directed toward the substrate in such a manner as to assist the hydride transfer by dipole–dipole repulsion. Our molecular dynamic calculations using enzyme X-ray coordinates and pyruvate at the active site show, however, that the amide bond swings through an arc of more than 50° such that the carbonyl oxygen alternates between the A- and B-side of the 1,4-dihydropyridine ring.

AM1 calculations of reaction trajectories have been carried out in order to determine the importance of the various functionalities at the active site to the rate of the reduction of a carbonyl function. For this purpose the functional groups were brought into place in space as seen in the X-ray structure of the dogfish enzyme with the *quasi*-boat structure for the dihydronicotinamide with $\alpha_N = 5°$ and $\alpha_C = 15°$ (Chart VI) and an *anti* antiperiplanar conformation of NADH. Our results are as follows. When the protonated guanidino group of ARG 106 is present, general-acid catalysis by protonated HIS 193 is about as effective in the catalysis of the hydride transfer as is complete pre-protonation catalysis. The computed trajectory suggests a very late transition

(24) Raber, D. J.; Rodriguez, W. J. *J. Am. Chem. Soc.* **1985**, *107*, 4146.

(25) There is also the possibility that differences in solvation could account for the preference for binding the reduced form of the cofactor. MD simulations of DHFR using the free energy perturbation method indicate that the observed 10^2 factor of relative binding of NADPH over $NADP^+$ could be due to the calculated differences in solvation free energy of 2–3 kcal/mol. See: Cummins, P. L.; Ramnarayan, K.; Singh, U. C.; Gready, J. E. *J. Am. Chem. Soc.* **1991**, *113*, 8247.

(26) Dalziel, K. In *The Enzymes*, 3rd ed.; Boyer, P. D., Ed.; Academic Press: New York, 1975; Vol. XI, pp 1–59.

(27) Deng, H.; Zheng, J.; Sloan, D.; Burgner, J.; Callender, R. *Biochemistry* **1992**, *31*, 5085.

(28) (a) Donkersloot, M. C. A.; Buck, H. M. *J. Am. Chem. Soc.* **1981**, *103*, 6554. (b) Beijer, N. A.; Buck, H. M.; Sluyterman, L. A. A.; Meijer, E. M. *Biochem. Biophys. Acta* **1990**, *1039*, 227.

state (Chart XIII) for general-acid proton transfer to substrate oxygen ($-\alpha = 0.9$) and a midway transition state for hydride transfer to carbon. Such a mechanism has much of the advantage of specific acid catalysis but retains the essential feature of general-acid catalysis being able to localize the proton at the active site. These results are much like the recent proposal of late transition state for protonation in the concerted enzymatic general-acid general-base catalysis of carbon acid enolization.[29] Wilkie and Williams[30] have recently shown, by use of a MAR[31] diagram, that this type of transition state is indeed to be expected. In this paper, we have included the protonated guanidine of ARG 106, since it is apparent from mutagenesis studies on *B. stearothermophilus* lactate dehydrogenase,[8] as well as from resonance Raman measurements with native porcine heart lactate dehydrogenase,[32] that the guanidine residue is very important to the mechanism of lactate dehydrogenases.

Our MD simulations with the dogfish enzyme indicate that the protonated imidazole of HIS 193 is required for complexing the substrate in the correct orientation for reduction by NADH. The hydrogen bond between pyruvate keto oxygen and imidazolium ion proton is tenacious throughout the dynamics range. The same observation pertains to the bifurcated hydrogen bond (salt bridge) between ARG 169 and the carboxylate of pyruvate, as long as the essential HIS 193 is protonated. In addition, ARG 106 adds another hydrogen bond to the substrate carbonyl oxygen. When HIS 193 is protonated, the substrate carbonyl carbon is in van der Waals contact with H_R of the dihydronicotinamide (Figure 9). Upon dissociation of protonated imidazole of HIS 193, the substrate turns around in the active site such that the bifurcated hydrogen bonds of its carboxylate with ARG 169 are broken (see Chart XI). In place, single hydrogen bonds from the substrate carboxylates to both ARG 169 and THR 245 are created, and the carbonyl oxygen engages in a reinforced hydrogen bond with ARG 106. The methyl group of pyruvate approaches the HIS 193 imidazole group and the carbonyl carbon becomes distant from the nicotinamide C4 hydrogen.

Weakly polar interactions involving C–H hydrogen bonds[33] have been implicated in dihydrofolate reductase catalysis. The X-ray structure data for the enzyme[14c] establishes very close contacts between oxygen atoms in dihydrofolate reductase and the hydrogens on C2, C4, and C6 of the nicotinamide ring. It was suggested that these contacts are C–H–O hydrogen bonds. Such hydrogen bonds were postulated to stabilize the positively charged $NADP^+$. Evidence for this is circumstantial, and calculations do not seem to bear out this notion. Indeed, C–H bonds in aromatic rings are generally not polarized to any significant extent. An alternate and more reasonable role for the amide carbonyl oxygens of ILE 13 and ALA 97 and the hydroxyl oxygen of THR 45 is to hydrogen bond to water molecules in the apoenzyme in order to maintain the tertiary structure of the active site. We were prompted to examine this possibility, using the coordinates for apolactate dehydrogenase from dogfish. In the dogfish enzyme, the carbonyl oxygen of VAL 136 and the hydroxyl oxygen of THR 245 have close contacts with hydrogens on C2 and C5 of the nicotinamide ring. The carbonyl oxygen of VAL 136 is hydrogen bonded to water molecule 473 in the apoenzyme and this water molecule is part of a hydrogen bonded network which fills the space vacated by cofactor on formation of the apoenzyme (see Results). These water molecules are retained in the course of MD simulations with apoenzyme for over 100 ps. If these are removed, prior to calculation of dynamic trajectories, the changes in the active site are dramatic, to the effect of closing the active site (see Results and Figure 11). The motions of the protein in binding cofactor and releasing most of the water have been carefully illustrated by Rossmann and colleagues.[14b] We suggest that the role for the polar environment which is peripheral to the nicotinamide ring in the enzyme is the preservation of the active site environment in the apoenzyme by hydrogen bonding to a stable water structure.

Acknowledgment. This research was supported by grants from the National Institute of Health, the National Science Foundation, and the Office of Naval Research. Ö. A. acknowledges a NATO Science fellowship.

(29) This compares with the mechanism suggested for enzyme catalyzed carbon acid ionizations, see: Gerlt, J. A.; Kozarich, J. W.; Kenyon, G. L.; Gassman, P. G. *J. Am. Chem. Soc.* **1991**, *113*, 9667. Gerlt, J. A.; Gassman, P. G. *J. Am. Chem. Soc.* **1992**, *114*, 5928.

(30) Wilkie, J.; Williams, I. H. *J. Am. Chem. Soc.* **1992**, *114*, 5423.

(31) Bruice, T. C. *Annu. Rev. Biochem.* **1976**, *45*, 331.

(32) Deng, H.; Zheng, J.; Burgner, J.; Callender, R. *Proc. Natl. Acad. Sci. U.S.A.* **1989**, *86*, 4484.

(33) For a review, see: Burley, S. K.; Petsko, G. A. *Adv. Proteins Chem.* **1988**, *39*, 125.